Rational Synthesis of High Nuclearity Mo/Fe/S Clusters: The Reductive Coupling Approach in the Convenient Synthesis of $(Cl_4\text{-cat})_2Mo_2Fe_6S_8(PR_3)_6$ [R = Et, ^{n}Pr, ^{n}Bu] and the New $[(Cl_4\text{-cat})_2Mo_2Fe_2S_3O(PEt_3)_3Cl]\cdot 1/2(Fe(PEt_3)_2(MeCN)_4)$ and $(Cl_4\text{-cat})_2Mo_2Fe_3S_5(PEt_3)_5$ Clusters

Jaehong Han, Markos Koutmos, Saleem Al Ahmad, and Dimitri Coucouvanis*

Department of Chemistry, The University of Michigan, Ann Arbor, Michigan 48109-1055

Received May 9, 2001

A general method for the synthesis of high nuclearity Mo/Fe/S clusters is presented and involves the reductive coupling of the $(Et_4N)_2[(Cl_4\text{-cat})MoOFeS_2Cl_2]$ (**I**) and $(Et_4N)_2[Fe_2S_2Cl_4]$ (**II**) clusters. The reaction of **I** and **II** with $Fe(PR_3)_2Cl_2$ or sodium salts of noncoordinating anions such as $NaPF_6$ or $NaBPh_4$ in the presence of PR_3 (R = Et, ^{n}Pr, or ^{n}Bu) affords $(Cl_4\text{-cat})_2Mo_2Fe_6S_8(PR_3)_6$ [R = Et (**IIIa**), ^{n}Pr (**IIIb**), ^{n}Bu (**IIIc**)], $Fe_6S_6(PEt_3)_4Cl_2$ (**IV**) and $(PF_6)[Fe_6S_8(P^nPr_3)_6]$ (**V**) as byproducts. The isolation of $(Et_4N)[Fe(PEt_3)Cl_3]$ (**VI**), NaCl, and $SPEt_3$ supports a reductive coupling mechanism. Cluster **IV** and **V** also have been synthesized by the reductive self-coupling of compound **II**. The reductive coupling reaction between **I** and **II** by PEt_3 and $NaPF_6$ in a 1:1 ratio produces the $(Et_4N)_2[(Cl_4\text{-cat})Mo(L)Fe_3S_4Cl_3]$ clusters [L = MeCN (**VIIa**), THF (**VIIb**)]. The hitherto unknown $[(Cl_4\text{-cat})_2Mo_2Fe_2S_3O(PEt_3)_3Cl]^+$ cluster (**VIII**) has been isolated as the 2:1 salt of the $(Fe(PEt_3)_2(MeCN)_4)^{2+}$ cation after the reductive self-coupling reaction of **I** in the presence of $Fe(PEt_3)_2Cl_2$. Cluster **VIII** crystallizes in the monoclinic space group $P2_1/c$ with $a = 11.098(3)$ Å, $b = 22.827(6)$ Å, $c = 25.855(6)$ Å, $\beta = 91.680(4)°$, and $Z = 4$. The formal oxidation states of metal atoms in **VIII** have been assigned as Mo^{III}, Mo^{IV}, Fe^{II}, and Fe^{III} on the basis of zero-field Mössbauer spectra. The $Fe(PEt_3)_2(MeCN)_4$ cation of **VIII** is also synthesized independently, isolated as the BPh_4^- salt (**IX**), and has been structurally characterized. The reductive coupling of compound **I** also affords in low yield the new $(Cl_4\text{-cat})_2Mo_2Fe_3S_5(PEt_3)_5$ cluster (**X**) as a byproduct. Cluster **X** crystallizes in the monoclinic space group $P2_1/n$ with $a = 14.811(3)$ Å, $b = 22.188(4)$ Å, $c = 21.864(4)$ Å, $\beta = 100.124(3)°$, and $Z = 4$ and the structure shows very short Mo−Fe, Fe−Fe, Mo−S, Fe−S bonds. The oxidation states of the metal atoms in this neutral cluster (**X**) have been assigned as $Mo^{IV}Mo^{III}Fe^{II}Fe^{II}Fe^{III}$ based on zero-field Mössbauer and magnetic measurement. All Fe atoms are high spin and two of the three Fe−Fe distances are found at 2.4683(9) Å and 2.4721(9) Å.

Introduction

Interest in the syntheses, structures, and reactivities of Mo/Fe/S clusters derives from the apparent involvement of such clusters in biological dinitrogen fixation[1] and their possible importance in hydrodesulfurization catalysis.[2] Since the structures of the nitrogenase cofactor (FeMoco) and the P cluster were revealed[3] (Figure 1), the synthesis and structures of high nuclearity Mo/Fe/S clusters has received particular attention. Among the plethora of Mo/Fe/S and Fe/S clusters known and well-characterized are included the $[Mo_2Fe_7S_8(SR)_{12}]^{3-}$,[4] $[Mo_2Fe_6S_8(SR)_9]^{3-}$,[5] and $MoFe_4S_6(PEt_3)_4Cl$[6] clusters. These compounds have been obtained by self-assembly methods, and their formation is determined by thermodynamic stability in the absence of kinetic constraints.

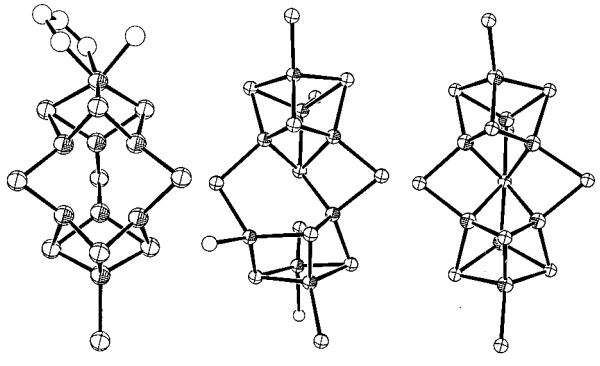

Figure 1. Structure of FeMoco and the P clusters.[1e] The P^N cluster is the two-electron reduced form of the P^{OX} cluster. The spheres with octant shading present Fe atoms and those without shading present S atoms. Terminal carbon, nitrogen, and oxygen ligands are shown as simple spheres.

(1) (a) Howard, J. B.; Rees, D. C. *Chem. Rev.* **1996**, *96*, 2965 and references therein. (b) Coucouvanis, D.; Han, J.; Demadis, K. D. *J. Inorg. Biochem.* **1999**, *74*, 18. (c) Coucouvanis, D. *J. Biol. Inorg. Chem.* **1996**, *1*, 594. (d) Peters, J. W.; Stowell, M. H. B.; Soltis, S. M.; Finnegan, M. G.; Johnson, M. K.; Rees, D. C. *Biochemistry* **1997**, *36*, 1181. (e) Mayer, S. M.; Lawson, D. M.; Gormal, C. A.; Roe, S. M.; Smith, B. E. J. Mol. Biol. **1999**, *292*, 871.

(2) Curtis, D. M. In *Transition metal sulfur chemistry: biological and industrial significance*; Stiefel, E. I.; Matsumoto, K., Eds.; ACS Symposium Series 653, American Chemical Society: Washington, DC, 1996; pp 154−175 and references therein.

(3) Kim, J.; Rees, D. C. *Science* **1992**, *257*, 1677.

(4) (a) Wolff, T. E.; Power, P. P.; Frankel, R. B.; Holm. R. H. *J. Am. Chem. Soc.* **1980**, *102*, 4694. (b) Palermo, R. E.; Power, P. P.; Holm, R. H. *Inorg. Chem.* **1982**, *21*, 173.

(5) (a) Christou, G.; Garner, C. D.; Mabbs, F. E. *J. Chem. Soc., Chem. Commun.* **1978**, 740. (b) Christou, G.; Garner, C. D.; Mabbs, F. E.; Drew, M. G. B. *J. Chem. Soc., Chem. Commun.* **1979**, 91. (c) Wolff, T. E.; Berg, J. M.; Hodgson, K. O.; Frankel, R. B.; Holm. R. H. *J. Am. Chem. Soc.* **1979**, *101*, 4140.

10.1021/ic0104914 CCC: $20.00 © 2001 American Chemical Society
Published on Web 10/10/2001

In polynuclear M/S chemistry, examples of product diversity determined by reagent ratios are found in the syntheses of $Fe_nS_6(PR_3)_4Cl_{n-4}$ (R = Et or Cy (cyclohexyl), n = 6, 7, and 8) clusters.[7,8] The importance of the counterion in stabilizing clusters with different nuclearity (at least in the solid state) is demonstrated in the synthesis and isolation of the $(^nBu_4N)_2[Fe_4S_4Cl_4]$ and $(Et_4N)_3[Fe_6S_6Cl_6]$ clusters.[9] Finally, ligands with different electronic and/or steric properties lead to different products as well.[10] In all these "spontaneous assembly" reactions, it is almost impossible to predict the stoichiometry or control the structure of the products. This is aptly illustrated in the synthesis of the $[Na_2Fe_{18}S_{30}]^{8-}$ cluster[11] from the simple reagents of $FeCl_3$, Li_2S, and Na[PhNC(O)Me].

The high nuclearity metal−sulfur (Mo/Fe/S and Fe/S) clusters may adopt various structures, as a result of nearly equi-energetic thermodynamic stabilities of various possible structures. Further complications may arise as results of structural interconversions in the absence of kinetic barriers. Interconversions may be promoted by small environmental differences, such as changes in solvent, ligand, or counterion, which may stabilize various structures in their respective shallow energy minima. The unprecedented structures of the FeMoco and P clusters (Figure 1), in the MoFe protein of nitrogenase, may indeed be due to the fact that these clusters owe their existence to uniquely stabilizing, protein environments.

In our studies, concerned with the rational synthesis of Fe/S and Mo/Fe/S clusters, we have developed synthetic methodology for the stepwise synthesis of larger clusters that include $[(Fe_4S_4)_2S]^{2+}$ and the $[(MoFe_3S_4)_2X]^{4+}$ (X = S, O) clusters.[12] These clusters are obtained by substitution of halide terminal ligands in the $[Fe_4S_4]^{2+}$ and $[MoFe_3F_4]^{3+}$ clusters by bridging sulfido ligand (Figure 2A). In the synthesis of the $(Cl_4\text{-cat})_2Mo_2Fe_6S_8(PEt_3)_6$ cluster (**IIIa**),[13] terminal Cl^- ligands are removed from the $(Et_4N)_2[(Cl_4\text{-cat})Mo(MeCN)Fe_3S_4Cl_3]$ cluster (**VIIa**)[14] by precipitation of NaCl in the presence of trialkylphosphine ligands.[15] The synthesis of **IIIa** is hindered by the time-consuming, cumbersome, synthesis of the **VIIa** precursor. Unfortunately, a convenient synthesis of the tetranuclear, heterometallic, $MoFe_3S_4$ cubanes has not been developed to date. This is in contrast to the $[Fe_4S_4]^{2+}$ cubanes which are readily obtained by the reductive coupling of $[Fe_2S_2]^{2+}$ dimers.[16] Condensation of the $Fe_2S_2(CO)_6$ dimer[17] similarly affords various high nuclearity clusters including the $Fe_4S_4(CO)_{12}$ cuboidal cluster.[18]

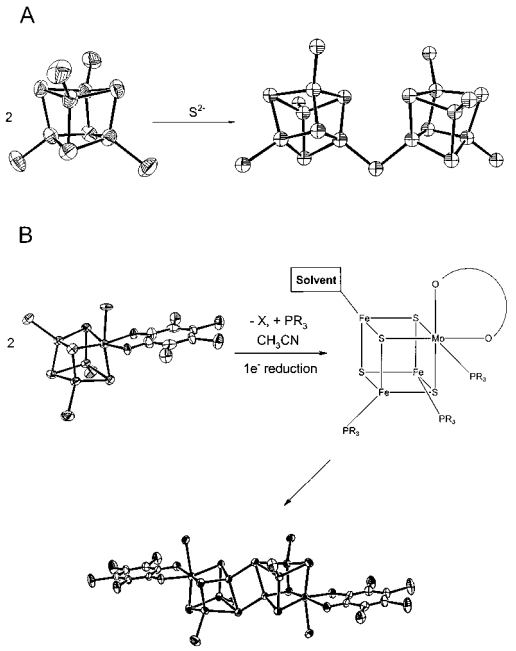

Figure 2. Synthetic methodology used for building high nuclearity Fe/S and Mo/Fe/S clusters. A. Coupling of two $[Fe_4S_4]^{2+}$ units by ligand substitution.[12] B. Coupling of two $[MoFe_3S_4]^{3+}$ units by ligand substitution and cluster reduction.[15]

In this paper we report on a general procedure for the synthesis of the heteronuclear $MoFe_3S_4$ cubanes and derivatives. This procedure is based on the reductive coupling of the $(Et_4N)_2[(Cl_4\text{-cat})MoOFeS_2Cl_2]$, (**I**)[19] and $(Et_4N)_2[Fe_2S_2Cl_4]$ (**II**)[20] dimers. The general utility of the reductive coupling approach is illustrated in the synthesis of the $[(Cl_4\text{-cat})(L)MoFe_3S_4Cl_3]^{2-}$ (L = CH_3CN, (**VIIa**); THF, (**VIIb**)), the $[(Cl_4\text{-cat})(L)Mo_2Fe_2S_3O(PEt_3)_3Cl]^{2-}$ (**VIII**) and the $(Cl_4\text{-cat})_2Mo_2Fe_6S_8(PR_3)_6$ [R = Et (**IIIa**), ^{n}Pr (**IIIb**), ^{n}Bu (**IIIc**)]. The synthesis and physical properties of the new $(Cl_4\text{-cat})_2Mo_2Fe_3S_5(PEt_3)_5$ cluster, (**X**), obtained as a minor byproduct, also are reported.

Understanding the scope of reductive assembly and oxidative disassembly of metal/sulfur clusters is of particular importance to biology. Recently, exciting findings have been reported on Fe/S cluster biosynthesis and the importance of cluster trans-

(6) (a) Nordlander, E.; Lee, S. C.; Cen, W.; Wu, Z. Y.; Natoli, C. R.; Cicco, D.; Filipponi, A.; Hedman, B.; Hodgson, K. O.; Holm, R. H. *J. Am. Chem. Soc*. **1993**, *115*, 5549. (b) Cen, W.; MacDonnell, F. M.; Scott, M. J.; Holm, R. H. *Inorg. Chem*. **1994**, *33*, 5809.
(7) (a) Noda, I.; Snyder, B. S.; Holm. R. H. *Inorg. Chem*. **1986**, *25*, 3851. (b) Snyder, B. S.; Holm. R. H. *Inorg. Chem*. **1988**, *27*, 2339. (c) Snyder, B. S.; Reynolds, M. S.; Noda, I.; Holm, R. H. *Inorg. Chem*. **1988**, *27*, 595. (d) Snyder, B. S.; Reynolds, M. S.; Papaefthymiou, G. C.; Frankel, R. B.; Holm, R. H. *Polyhedron* **1991**, *10*, 203.
(8) (a) Goh, C.; Segal, B. M.; Huang, J.; Long, J. R.; Holm, R. H. *J. Am. Chem. Soc*. **1996**, *118*, 11844. (b) Cai, L.; Segal, B. M.; Long, J. R.; Scott, M. J.; Holm, R. H. *J. Am. Chem. Soc*. **1995**, *117*, 8863.
(9) (a) Kanatzidis, M. G.; Dunham, W. R.; Hagen, W. R.; Coucouvanis, D. *Chem. Comm*. **1984**, 356. (b) Coucouvanis, D.; Kanatzidis, M. G.; Dunham, W. R.; Hagen, W. R. *J. Am. Chem. Soc*. **1984**, *106*, 7998. (c) Kanatzidis, M. G.; Hagen, W. R.; Dunham, W. R.; Lester, R. K.; Coucouvanis, D. *J. Am. Chem*. **1985**, *107*, 953. (d) Kanatzidis, M. G.; Salifoglou, A.; Coucouvanis, D. *J. Am. Chem. Soc*. **1985**, *107*, 3358. (e) Salifoglou, A.; Kanatzidis, M. G.; Coucouvanis, D. *Chem. Commun*. **1986**, 559. (f) Kanatzidis, M. G.; Salifoglou, A.; Coucouvanis, D. *Inorg. Chem*. **1986**, *25*, 2460. (g) Saak, W.; Henkel, G.; Pohl, S. *Angew. Chem., Int. Ed. Engl*. **1984**, *23*, 150. (h) Saak, W.; Pohl, S. *Z. Naturforsch., B.; Anorg. Chem., Org. Chem*. **1985**, *40b*, 1105.
(10) Chen, C.; Wen, T.; Li, W.; Zhu, H.; Chen, Y.; Liu, Q.; Lu, J. *Inorg. Chem.* **1999**, *38*, 2375.
(11) (a) You, J.-F.; Papaefthymiou, G. C.; Holm, R. H. *J. Am. Chem. Soc*. **1992**, *114*, 2697. (b) You, J.-F.; Snyder, B. S.; Papaefthymiou, G. C.; Holm, R. H. *J. Am. Chem. Soc*. **1990**, *112*, 1067. (c) You, J.-F.; Snyder, B. S.; Holm. R. H. *J. Am. Chem. Soc*. **1988**, *110*, 6589.
(12) (a) Coucouvanis, D.; Challen, P. R.; Koo, S.-M.; Davis, W. M.; Butler, W.; Dunham, W. R. *Inorg. Chem*. **1989**, *28*, 4181. (b) Challen, P. R.; Koo, S.-M.; Dunham, W. R.; Coucouvanis, D. *J. Am. Chem. Soc*. **1990**, *112*, 2455. (c) Huang, J.; Mukerjee, S.; Segal, B. M.; Akashi, H.; Zhou, J.; Holm, R. H. *J. Am. Chem. Soc*. **1997**, *119*, 8662. (d) Huang, J.; Goh, C.; Holm. R. H. *Inorg. Chem*. **1997**, *36*, 356. (e) Huang, J.; Holm. R. H. *Inorg. Chem*. **1998**, *37*, 2247.
(13) (a) $Cl_4\text{-cat}H_2$ = tetrachlorocatechol ($Cl_4C_6O_2H_2$), (b) Cl_4-cat = tetrachlorocatecholate ($Cl_4C_6O_2$).
(14) Mosier, P. E. Thesis, University of Michigan, 1994.
(15) Demadis, K. D.; Campana, C. F.; Coucouvanis, D. *J. Am. Chem. Soc*. **1995**, *117*, 7832.
(16) Wong, G. B.; Bobrik, M. A.; Holm, R. H. *Inorg. Chem*. **1978**, *17*, 578.
(17) (a) King, R. B.; Bitterwolf, T. E. *Coord. Chem. Rev*. **2000**, *206−207*, 563. (b) Ferrer, M.; Reina, R.; Rossell, O.; Seco, M. *Coord. Chem. Rev*. **1999**, *193−195*, 619. (c) Day, V. W.; Lesch, D. A.; Rauchfuss, T. B. *J. Am. Chem. Soc*. **1982**, *104*, 1290.
(18) Bogan, L. E., Jr.; Lesch, D. A.; Rauchfuss, T. B. *J. Organomet. Chem.* **1983**, *250*, 429.
(19) Coucouvanis, D.; Al-Ahmad, S.; Kim, C. G.; Mosier, P. E.; Kampf, J. W. *Inorg. Chem*. **1993**, *32*, 1533.
(20) Do, Y.; Simhon, E. D.; Holm, R. H. *Inorg. Chem*. **1983**, *22*, 3809.

formations in gene expression.[21] The oxidative disassembly of an $[Fe_4S_4]^{2+}$ cluster to $[Fe_2S_2]^{2+}$ cluster in *Escherichia coli* FNR (fumarate nitrate reductase regulator)[22] and the reductive sequential assembly of $[Fe_2S_2]^{2+}$ cluster to an $[Fe_4S_4]^{2+}$ cluster in IscU from *Azotobacter vinelandii*[23] are biological examples of redox-based cluster interconversions.

Experimental Section

General. All experiments and reactions were carried out under a dinitrogen atmosphere using standard Schlenk line techniques or in an inert atmosphere glovebox. All solvents were distilled under dinitrogen and nitrogen gas was bubbled through each before use in the glovebox. Acetonitrile was predried over oven-dried molecular sieves and distilled over CaH_2. Ethyl ether and THF were predried over Na ribbon and further purified by the sodium−benzoketyl method. Dichloromethane was distilled over P_2O_5. Tetrachlorocatechol (Cl_4−$catH_2$) (Lancaster) was dissolved in ethyl ether, and the concentrated solution was treated with activated charcoal (Aldrich). After a few hours, the mixture was filtered by gravity filtration and the process continued until the ether solution contained no dark brown color. Once the color of the diethyl ether solution became lighter, the solvent was removed by nitrogen purging, and the residue was dried under vacuum. Anhydrous $FeCl_2$, PEt_3, P^nPr_3, P^nBu_3, $NaPF_6$, and $NaBPh_4$ were purchased from STREM or Aldrich and used without further purification. $(NH_4)_2[MoO_2S_2]$,[24] $(Et_4N)_2[FeCl_4]$,[25] $(Et_4N)[FeCl_4]$, and $(Et_4N)_2[Fe_2S_2Cl_4]$ (**II**)[20] were synthesized according to published methods after slight modifications. $Fe(PEt_3)_2Cl_2$ was prepared from a 1:2 molar ratio of $FeCl_2$ and PEt_3 in THF.

FT-IR spectra were collected on a Nicolet DX V. 4.56 FT-IR spectrometer in KBr pellets and the spectra were corrected for background. Elemental analyses were performed by the Microanalytical Laboratory at the University of Michigan. The data were corrected using acetanilide as a standard. Electronic spectra were recorded on a Varian CARY 1E UV−Visible spectrometer. Mössbauer spectra were obtained with the high-sensitivity Mössbauer spectrometer in the Biophysics department at the University of Michigan.[26] All the Mössbauer measurements were carried out at 125 K in zero applied magnetic field. The source was ^{57}Co in a Rh matrix, and the isomer shift was reported versus Fe metal at room temperature. The magnetic susceptibility measurements were carried out on a MPMS SQUID magnetometer, and the data were corrected for diamagnetic contributions. FAB^+ mass spectra were obtained at the University of Michigan Mass Spectroscopy Laboratory with a 3-nitrobenzoyl alcohol matrix.

The compounds of primary interest are designated as follows:

$$(Et_4N)_2[(Cl_4\text{-cat})MoOFeS_2Cl_2] \quad (I)$$

$$(Et_4N)_2[Fe_2S_2Cl_4] \quad (II)$$

$$[(Cl_4\text{-cat})_2Mo_2Fe_6S_8(PEt_3)_6] \quad (IIIa)$$

$$[(Cl_4\text{-cat})_2Mo_2Fe_6S_8(P^nPr_3)_6] \quad (IIIb)$$

$$[(Cl_4\text{-cat})_2Mo_2Fe_6S_8(P^nBu_3)_6] \quad (IIIc)$$

$$[Fe_6S_6(PEt_3)_4Cl_2] \quad (IV)$$

$$(PF_6)[Fe_6S_8(P^nPr_3)_6] \quad (V)$$

$$(Et_4N)[Fe(PEt_3)Cl_3] \quad (VI)$$

$$(Et_4N)_2[(Cl_4\text{-cat})Mo(MeCN)Fe_3S_4Cl_3] \quad (VIIa)$$

$$(Et_4N)_2[(Cl_4\text{-cat})Mo(THF)Fe_3S_4Cl_3] \quad (VIIb)$$

$$[(Cl_4\text{-cat})_2Mo_2Fe_2S_3O(PEt_3)_3Cl]\cdot 1/2(Fe(PEt_3)_2(MeCN)_4) \quad (VIII)$$

$$(B\ Ph_4)[Fe(PEt_3)_2(MeCN)_4] \quad (IX)$$

$$[(Cl_4\text{-cat})_2Mo_2Fe_3S_5(PEt_3)_5] \quad (X)$$

$(Et_4N)_2[MoO_2S_2FeCl_2]$. To a solution of $(Et_4N)_2[FeCl_4]$ (1 g, 2.18 mmol) in MeCN (80 mL) was added $(NH_4)_2[MoO_2S_2]$ (0.5 g, 2.19 mmol). After being stirred for 40 min, the reaction mixture was filtered to remove H_4NCl. The filtrate was diluted with 100 mL of diethyl ether to produce an orange powder and red crystalline $(Et_4N)_2[MoO_2S_2FeCl_2]$ (900 mg, 1.55 mmol, 71.1%). FT-IR (KBr, cm^{-1}) ν(C−H of Et_4N) 2986(m) and 2946(w), ν(Mo≡O) 899(s) and 873(s), ν(μ_2-S of Mo−S−Fe) 452(m). $(Ph_4P)_2[MoO_2S_2FeCl_2]$ was prepared using the same method in 70% yield. FT-IR (KBr, cm^{-1}) ν(Mo≡O) 902(s) and 877(s), ν(μ_2-S of Mo−S−Fe) 453(m). Anal. Calcd for $MoFeCl_2S_2P_2O_2C_{48}H_{40}$ (MW 997.43): C, 57.8; H, 4.05; Fe, 5.59. Found: C, 58.7; H, 4.07, Fe, 5.31.

$(Et_4N)_2[(Cl_4\text{-cat})Mo(O)S_2FeCl_2]$ (I). Cl_4-$catH_2$ (0.4 g, 1.61 mmol) was added to a solution of $(Et_4N)_2[Cl_2FeS_2MoO_2]$ (0.9 g,1.55 mmol) in MeCN (20 mL), which produced an immediate color change from orange to green. The reaction mixture was allowed to stir for 1 h, and diethyl ether (60 mL) was deposited carefully over the MeCN filtrate after filtration. The assembly was cooled to 0 °C and after standing for 1 day produced greenish black rhombic crystals (1.0 g, 1.24 mmol, 80% yield). FT-IR (KBr, cm^{-1}) ν(C−H of Et_4N) 2984(m) and 2946(w), ν(Cl_4-cat) 1437(s) and 1252(m, C−O), ν(Mo≡O) 939, ν(Mo−Cl_4-cat) 564, ν(μ_2-S of Mo−S−Fe) 446(m). UV−Vis (MeCN, nm) 630, 460, 360. Anal. Calcd for $MoFeCl_6S_2O_3N_2C_{22}H_{40}$ (MW. 809.198): C, 32.65; H, 4.98; N, 3.46. Found: C, 32.70; H, 5.03; N, 3.22. Magnetic moment (powder, BM) 5.413(300 K), 4.741(5 K). Cyclic voltammetry[27] (MeCN, 0.1 M of Et_4NPF_6) −1.1(irr), −1.45(qr), 0.06(qr).

$(Cl_4\text{-cat})_2Mo_2Fe_6S_8(PEt_3)_6$ (IIIa). A mixture of $(Et_4N)_2[(Cl_4$-$cat)MoOS_2FeCl_2]$ (**I**) (809 mg, 1 mmol), $(Et_4N)_2[Fe_2S_2Cl_4]$ (**II**) (578 mg, 1 mmol), and $Fe(PEt_3)_2Cl_2$ (2.178 g, 6 mmol) was dissolved into 30 mL of MeCN to give a black solution. A black solid precipitated within hours, and the reaction mixture was stirred for 1 day. The known $Fe_6S_6(PEt_3)_4Cl_2$ cluster[7] (120 mg, 0.112 mmol, 33.6% from **II**) was isolated upon filtration of the reaction mixture. The filtrate was kept for 1 day, and a black powder was deposited on the bottom of the flask. The product, isolated by decanting the solution, was identified as $(Cl_4$-$cat)_2Mo_2Fe_6S_8(PEt_3)_6$ (**IIIa**) by IR and CHN analysis (200 mg, 0.1 mmol, 20%).

$(Cl_4\text{-cat})_2Mo_2Fe_6S_8(P^nPr_3)_6$ (IIIb). Method A. To a stirred solution of 1.5 g (1.86 mmol) of $(Et_4N)_2[(Cl_4$-$cat)MoOS_2FeCl_2]$ and 0.98 g (1.86 mmol) of $(Et_4N)_2[Fe_2S_2Cl_4]$ in 25 mL of MeCN was added dropwise 2.1 g (2.62 mL; 13.02 mmol) of P^nPr_3 via a syringe followed by a solution of 1.90 g (11.16 mmol) of $NaPF_6$ in 5 mL of MeCN. The reaction mixture was stirred overnight, and the resulting dark-brown solution was allowed to stand for a few hours in the glovebox at room temperature and then filtered through Celite. The precipitate was washed with additional MeCN and hexanes and extracted with dichloromethane, leaving a white residue (NaCl). Hexanes were allowed to diffuse slowly into the dichloromethane extract to afford the product as 650 mg (0.27 mmol, 29%) of black crystals. Anal. Calcd for $Mo_2Fe_6O_4P_6S_8Cl_{12}C_{68}H_{130}$ (**III**·$2CH_2Cl_2$ MW. 2406.33): C, 33.94; H, 5.44. Found: C, 33.79; H, 5.68. IR(KBr, cm^{-1})[28] 2962(s), 2931(m), 2896(w), 2872(m), 1438(vs), 1254(s), 1081(s), 976(s), 806(s), 780(m), 744(m), 735(m), 707(m), 525(m). UV−Vis (CH_2Cl_2, nm) 310. Cyclic voltammetry (1,2-dichloroethane, mV) −903 (qr), −550 (qr), −250 (qr), +202 (irr). EPR (frozen THF or CH_2Cl_2) silent.

(21) Beinert, H. *Eur. J. Biochem*. **2000**, *267*, 5657.
(22) Khoroshilova, N.; Beinert, H.; Kiley, P. J. *Proc. Natl. Acad. Sci. U.S.A.* **1995**, *92*, 2499.
(23) Agar, J. N.; Krebs, C.; Frazzon, J.; Hyunh, B. H.; Dean, D. R.; Johnson, M. K. *Biochemistry* **2000**, *39*, 7856.
(24) McDonald, J. W.; Frisen, G. D.; Resenhein, L. D.; Newton, W. E. *Inorg. Chim. Acta*. **1983**, *72*, 205.
(25) Gill, N. S.; Taylor, F. B. *Inorg. Synth*. **1967**, *9*, 136.
(26) Moon, N.; Coffin, C. T.; Steinke, D. C.; Sands, R. H.; Dunham, W. R. *Nucl. Inst. Methods Phys. Res. B.* **1996**, *119*, 555.

(27) All the cyclic voltammetry experiments were carried out with Pt working and Ag/AgCl reference electrode with 0.1M of $^nBu_4NPF_6$ electrolyte otherwise noted. The redox potentials were reported vs SCE. rev = reversible, qr = quasi-reversible, irr = irreversible.
(28) The peaks between 2800 and 3000 cm^{-1} are characteristic for the ^nPr group. Cl_4-cat shows a characteristic 1438 cm^{-1} peak.

Method B. A MeCN (30 mL) solution of $Fe(P^nPr_3)_2Cl_2$ (2.5 g, 5.6 mmol), $(Et_4N)_2[(Cl_4\text{-cat})MoOS_2FeCl_2]$ (**I**) (809 mg, 1 mmol), and $(Et_4N)_2[Fe_2S_2Cl_4]$ (**II**) (578 mg, 1 mmol) was prepared and agitated by stirring at ambient temperature for 1 day. The black precipitate that formed was isolated by filtration through a fine-porosity frit and washed with 5 mL of MeCN. This residue was extracted with dichloromethane, and a layer of hexane was deposited carefully. Upon standing, black crystals of $(Cl_4\text{-cat})_2Mo_2Fe_6S_8(P^nPr_3)_6$ (**IIIb**) (150 mg, 0.067 mmol, 13.4% yield) were obtained and identified by IR and CHN analysis.

$(Cl_4\text{-cat})_2Mo_2Fe_6S_8(P^nBu_3)_6$ (IIIc). The same method A (see above) was used with 0.5 g (0.94 mmol) of $(Et_4N)_2[(Cl_4\text{-cat})MoOS_2FeCl_2]$, 0.33 g (0.94 mmol) of $(Et_4N)_2[Fe_2S_2Cl_4]$, 0.88 g (6.51 mmol) of P^nBu_3, and 0.63 g of $NaPF_6$ in 20 mL of MeCN. A brown-colored powder was isolated by filtration and recrystallized from dichloromethane and hexanes to afford 200 mg (29% yield) of the product. Black rhombic crystals isolated were suitable for X-ray determination. FT-IR (KBr, cm^{-1}) 2957(s), 2928(s), 2869(m), 1436(s), 1377(m), 1254(m), 1094(w), 975(m), 903(m), 806(s), 780(m), 720(m), 525(m). UV−Vis (CH_2Cl_2, nm) 322. Anal. Calcd for $Mo_2Fe_6O_4P_6S_8Cl_{12}C_{86}H_{166}$ (**IIIa**·$2CH_2Cl_2$ MW 2658.99): C, 38.85; H, 6.29. Found: C, 38.74; H, 6.38. Magnetic susceptibility (solid): μ_{eff} (4 K) = 4.42 μ_B, μ_{eff} (300 K) = 5.02 μ_B.

$Fe_6S_6(PEt_3)_4Cl_2$ (IV). Method A. $(Et_4N)_2[Fe_2S_2Cl_4]$ (0.500 g, 0.865 mmol) was dissolved in acetonitrile (20 mL), and to the stirring solution was added PEt_3 (0.511 mL, 3.46 mmol) dropwise, followed by solid $NaPF_6$ (0.581 g, 3.46 mmol). After a few minutes, a black precipitate was observed. The solution was stirred overnight, and the solid was isolated by filtration, washed with excess acetonitrile, and extracted into dichloromethane (25 mL), leaving white NaCl on the frit. The solvent was removed under a nitrogen stream, yielding a black residue identified by FT-IR as $[Fe_6S_6(PEt_3)_4Cl_2]$ (**IVa**) (90 mg, 0.084 mmol, 29% yield). FT-IR (CsI, cm^{-1}): 2965 (m), 2932 (m), 2900 (m), 2871 (m), 1452 (m), 1407 (m), 1377 (m), 1257 (m), 1030 (s), 763 (s), 730 (m), 691 (w), 621 (m), 426 (w). Anal. Calcd for $Fe_6P_4S_6Cl_2C_{24}H_{60}$ (**IV** MW 1071.00): C, 26.91; H, 5.65. Found: C, 26.67; H, 5.60.

Method B. $(Et_4N)_2[Fe_2S_2Cl_4]$ (0.500 g, 0.865 mmol) and the $Fe(PEt_3)_2Cl_2$ reducing agent (1.26 g, 3.46 mmol) were dissolved together in acetonitrile (20 mL). A black precipitate was observed within a few minutes. After stirring overnight, the solid was isolated by filtration, washed with excess acetonitrile, and dried in vacuo on the filter. FT-IR analysis identified the product as $[Fe_6S_6(PEt_3)_4Cl_2]$ (**IVa**) (70 mg, 0.065 mmol, 23% yield).

$(PF_6)[Fe_6S_8(P^nPr_3)_6]$ (V). Method A. To a solution of $(Et_4N)_2[Fe_2S_2Cl_4]$ (0.5 g, 0.86 mmol) in 20 mL of MeCN was added P^nPr_3 (0.55 g, 3.4 mmol) via a syringe under vigorous stirring followed by a solution of $NaPF_6$ (0.57 g, 3.4 mmol). The resulting reaction mixture was stirred overnight. After filtration the crude solid was collected and recrystallized from CH_2Cl_2/hexanes to afford a black crystalline material (120 mg, 24% yield). FT-IR (KBr, cm^{-1}) 2957(vs), 2926(s), 2867(s), 1458(m), 1404(m), 1220(m), 1076(vs), 1037(s), 838(vs), 719(s). FAB^+-MS (NBA, *m*/*z*) 1553.0 [M − PF_6], 1392.5 [M − PF_6 − P^nPr_3], 1232.3 [M − PF_6 − $(P^nPr_3)_2$]. Anal. Calcd for $Fe_6S_6Cl_2F_6P_7C_{55}H_{128}$ (**V**·CH_2Cl_2, MW 1782.91) C, 37.05; H, 7.24. Found C, 37.09; H, 7.06. Magnetic susceptibility (solid): μ_{eff} (4 K) = 2.02 μ_B, μ_{eff} (300 K) = 3.16 μ_B

Method B. The preceding method was employed with 1.5 g (1.53 mmol) of $(Bu_4N)_2[Fe_4S_4Cl_4]$, 0.98 g (6.12 mmol) of P^nPr_3, and 1.03 g (6.12 mmol) of $NaPF_6$ in a total of 30 mL of MeCN. Recrystallization from dichloromethane/hexanes afforded 1.0 g of a crystalline product (74% yield). The product exhibited the same spectroscopic features as compound **V**.

$(Et_4N)[Fe(PEt_3)Cl_3]$ (VI). The compound was isolated from the reaction filtrate following the isolation of **IIIa**. Slow diffusion of diethyl ether into the MeCN reaction filtrate produced transparent rhombic crystals (200 mg, 0.49 mmol). The compound is extremely air-sensitive and in air turns black immediately with a smell of PEt_3. Anal. Calcd for $FeCl_3PNC_{14}H_{35}$ (MW 410.611): C, 40.95; H, 8.59; N, 3.41. Found: C, 40.76; H,8.79; N, 3.45. FT-IR (KBr, cm^{-1}) 3011(w), 2968(s), 2938(m), 2879(m), 1460(vs), 1405(s), 1185(s), 1050(m), 1034(m), 1006(m), 802(m), 772(m), 753(w), 693(w), 469(w). $FAB\text{-}MS^-$ (NBA, *m*/*z*) 280.1([M − $Et_4N]^+$). Magnetic susceptibility (solid): μ_{eff} (4 K) = 5.29 μ_B, μ_{eff} (300 K) = 5.58 μ_B. Mössbauer (boric acid, 125 K) δ = 0.84 mm/s ΔE_Q = 1.68 mm/s. The structure was identified by single-crystal X-ray crystallography.

$(Et_4N)_2[(Cl_4\text{-cat})Mo(THF)Fe_3S_4Cl_3]$ (VIIb). A solution of $(Et_4N)_2[(Cl_4\text{-cat})Mo(O)S_2FeCl_2]$ (2.43 g, 3.0 mmol), $(Et_4N)_2[Fe_2S_2Cl_4]$ (1.74 g, 3.0 mmol), and $NaPF_6$ (1.1 g, 6.5 mmol) in 60 mL of MeCN was stirred for 5 min and PEt_3 (0.45 mL, 3.0 mmol) was introduced slowly into the reaction flask. The reaction was stopped by filtration of the mixture after 20 h. A black residue was obtained after solvent evaporation and the IR spectrum of the crude product showed the presence of $(Et_4N)_2[(Cl_4\text{-cat})Mo(MeCN)Fe_3S_4Cl_3]$ (**VIIa**) and $(Et_4N)(PF_6)$ as well as an unknown byproduct. The residue was extracted with THF (3 × 20 mL) and crystallized by layering diethyl ether (100 mL) over the THF extract. After 1 day, the solution produced ca. 600 mg of the product contaminated with transparent crystalline $(Et_4N)(PF_6)$. The crude product was washed with MeOH (30 mL) and extracted with THF (30 mL). The recrystallization of the THF extract with ethyl ether (50 mL) afforded black needle crystals of $(Et_4N)_2[(Cl_4\text{-cat})Mo(THF)Fe_3S_4Cl_3]$ (**VIIb**) (350 mg, 0.325 mmol, 10.8% yield). FT-IR (KBr, cm^{-1}) 2977(w), 2870(w), 1431(s), 1254(m), 1171(w), 978(m), 807(m), 781(m), 544(w), 425(w), 411(w), 351(s).

$[(Cl_4\text{-cat})_2Mo_2Fe_2S_3O(PEt_3)_3Cl]\cdot 1/2(Fe(PEt_3)_2(MeCN)_4)$ (VIII). A mixture of $(Et_4N)_2[(Cl_4\text{-cat})Mo(O)S_2FeCl_2]$ (**I**) (0.809 g, 1.0 mmol) and $Fe(PEt_3)_2Cl_2$ (2.178 g, 6.0 mmol) was dissolved in 15 mL of MeCN, and the greenish black solution immediately turned dark purple. A black precipitate formed after a few hours and was isolated by filtration after 1 day. The product was washed with ethyl ether, and a tan-colored powder was isolated (200 mg, 0.128 mmol, 25% yield). FT-IR (KBr, cm^{-1}) 2966(w), 2935(w), 2877(w), 2248(w), 1443(s), 1254(m), 1038(m), 976(m), 806(m), 780(w), 766(w), 543(w), 530(w). UV−Vis (CH_2Cl_2, nm) 312, 465. (MeCN, nm) 320, 440. $FAB\text{-}MS^+$ (NBA, *m*/*z*) 1295.7 ([M − 2H]$^+$), 1279.6 ([M − $H_2O]^+$), $FAB\text{-}MS^-$ (NBA, *m*/*z*) 1259.2 ([M − $HCl]^-$). Anal. Calcd for $Mo_2Fe_{2.5}Cl_9S_3P_4O_5N_3C_{42}H_{69}$ (**II**·MeCN, MW. 1566.675): C, 32.20; H, 4.44; N, 2.68. Found: C, 32.05; H, 4.45; N, 2.64. Magnetic susceptibility (solid): μ_{eff} (4 K) = 5.33 μ_B, μ_{eff} (300 K) = 7.95 μ_B

$(BPh_4)_2[Fe(PEt_3)_2(MeCN)_4]$ (IX). A solution of $Fe(PEt_3)_2Cl_2$ (363 mg, 1 mmol) and $NaBPh_4$ (684 mg, 2 mmol) in 30 mL of MeCN was stirred for 1 h and filtered to remove NaCl. The dark beige filtrate was concentrated to 15 mL under a dinitrogen stream. Orange crystals formed (350 mg, 0.32 mmol, 88% yield) and were isolated by filtration. FT-IR (KBr, cm^{-1}) 3052 (m), 3036 (m), 2981 (m), 2938 (w), 2913 (m), 2251 (w), 1578 (m), 1574 (m), 1476 (m), 1456 (m), 1425 (m), 1259 (w), 1031 (m), 759 (m), 740 (s), 728 (s), 707 (s), 613 (m), 609 (m), 603 (m), 477 (w), 471 (w), 462 (w), 397 (s). ^1H NMR (400 MHz, DMSO, ppm) 7.16 (Ph, 16H), 6.91 (Ph, 16H), 6.78 (Ph, 8H), 5.75 (CH_2, 6H), 3.59 (CH_2, 6H), 1.63 (MeCN, 12H), 1.00 (CH_3, m, 18H). Anal. Calcd for $FeP_2N_4B_2C_{68}H_{82}$ (II, MW. 1094.820): C, 74.60; H, 7.55; N, 5.12. Found: C, 73.53; H, 7.57; N, 4.86. Magnetic susceptibility (solid): μ_{eff} (4 K) = 1.49 μ_B, μ_{eff} (300 K) = 5.33 μ_B.

$(Cl_4\text{-cat})_2Mo_2Fe_3S_5(PEt_3)_5$ (X). Method A. A mixture of $(Et_4N)_2[(Cl_4\text{-cat})(MeCN)MoFe_3S_4Cl_3]$ (**VIIa**) (1.0 g, 0.96 mmol) and $Fe(PEt_3)_2Cl_2$ (2 g, 5.51 mmol) was dissolved in MeCN (30 mL). The color of the reaction solution changed immediately from reddish black to dark greenish black. The reaction mixture was stirred for 1 day, and the precipitate was filtered using fine porous frit and washed with 5 mL of MeCN. Most of the precipitate was $(Cl_4\text{-cat})_2Mo_2Fe_6S_8(PEt_3)_6$ (**IIIa**) which was identified by IR and CHN analysis. The precipitate was extracted with 10 mL of diethyl ether and the extract was kept in the drybox for 20 days. Upon slow evaporation of the solvent, black rhombic crystals formed (10 mg, 6.0μmol, 1.25% yield based on Mo) as well as white needle shaped crystalline $SPEt_3$. FT-IR (KBr, cm^{-1}) 2964 (w), 2932 (w), 2901 (w), 2875 (w) (ν (PEt_3)), 1433 (s) (ν(Cl_4-cat)). Far-IR (KBr, cm^{-1}) 528 (vs), 470 (m), 453 (w), 438 (m), 410 (m), 377 (m), 326 (m). ^1H NMR (CD_2Cl_2, ppm) 8.6 (br. 2H), 8.05 (4H), 6.2 (4H), 5.55 (2H), 4.53 (4H), 3.69 (2H), 1.98 (2H), 1.82 (2H), 1.57 (4H), 1.27 (9H, Mo−PCH_2CH_3), 1.16 (9H, Mo−PCH_2CH_3), 0.89 (9H, Fe−PCH_2CH_3), 0.08 (18H, Fe−PCH_2CH_3), −2.02 (4H). UV−Vis (CH_2Cl_2, nm) 296 (sh), 600. Cyclic voltammetry (1,2-dichloroethane, 0.1 M $^nBu_4NPF_6$) 1580 mV (irr), 1220 mV (irr), 559 mV (qr), 125 mV (qr), −482 mV (irr), −728 mV (rev), −1013 mV (rev).

Table 1. Crystal Data and Structure Refinements for $(Cl_4\text{-cat})_2Mo_2Fe_6S_8(P^nBu_3)_6$ (**IIIc**), $(PF_6)[Fe_6S_8(P^nPr_3)_6]$ (**V**), $(Et_4N)[Fe(PEt_3)Cl_3]$ (**VI**), $(Et_4N)_2[(Cl_4\text{-cat})Mo(MeCN)Fe_3S_4Cl_3]$ (**VIIa**)

	IIIc	V	VI	VIIa
empirical formula	$C_{84}H_{162}Cl_8Fe_6Mo_2O_4P_6S_8\cdot(CH_2Cl_2)_2$	$C_{54}H_{126}F_6Fe_6P_7S_8$	$C_{14}H_{35}Cl_3FeNP$	$C_{24}H_{43}Cl_7Fe_3MoN_3O_2S_4$
formula weight	2658.87	1697.92	410.60	1045.49
wavelength, Å	0.71073	0.71073	0.71073	0.71073
crystal system	orthorhombic	trigonal	triclinic	monoclinic
space group	*Pccn*	*R*-3*c*	*P*-1	*Cm*
unit cell dimensions, Å and deg	$a = 16.7748(17)$	$a = 14.1878(14)$	$a = 12.003(4)$	$a = 13.090(3)$
	$b = 24.543(3)$		$b = 12.646(4)$	$b = 19.775(4)$
	$c = 29.360(3)$	$c = 66.895(9)$	$c = 13.851(5)$	$c = 9.6856(19)$
			$\alpha = 93.290(5)$	
			$\beta = 90.466(6)$	$\beta = 126.75(3)$
			$\gamma = 90.321$	
volume, Å^3	12088(2)	11661(2)	2099.0(12)	2009.1(7)
Z, calcd density, mg/mm^3	4, 1.461	6, 1.451	4, 1.299	2, 1.728
absorption coeff, mm^{-1}	1.423	1.496	1.169	2.068
F(000)	5504	5358	872	1054
crystal size, mm	0.38 × 0.36 × 0.22	0.28 × 0.26 × 0.22	0.24 × 0.20 × 0.20	0.30 × 0.30 × 0.40
θ range for data colln, deg	1.47 to 26.43	1.77 to 26.37	1.47 to 26.63	2.06 to 20.04
limiting indices	$-21 < h < 20$	$-17 < h < 17$	$-15 < h < 14$	$0 < h < 12$
	$-28 < k < 30$	$-17 < k < 17$	$-15 < k < 15$	$0 < k < 19$
	$-36 < l < 36$	$-83 < l < 83$	$-17 < l < 17$	$-9 < l < 7$
reflns collected/unique	120721/12410	34985/2669	20064/8521	2075/1044
R(int)	0.0602	0.0352	0.0665	0.0320
completeness to θ, %	99.8	100	96.8	100
data/restraints/parameters	12410/0/539	2669/0/131	8521/0/362	1042/2/247
goodness-of-fit on F^2	1.027	1.149	1.077	1.074
Final *R* indices [$I > 2\sigma(I)$]	R1 = 0.0761,	R1 = 0.0394,	R1 = 0.1415,	R1 = 0.0494,
	wR2 = 0.2054	wR2 = 0.0955	wR2 = 0.3927	wR2 = 0.1268
R indices (all data)	R1 = 0.0962,	R1 = 0.0424,	R1 = 0.1704,	R1 = 0.0542,
	wR2 = 0.2215	wR2 = 0.0969	wR2 = 0.4003	wR2 = 0.1354
R1 = 0.0542, wR2 = 0.1354				

Magnetic susceptibility (solid): μ_{eff} (4 K) = 3.14 μ_B, μ_{eff} (300 K) = 10.45 μ_B.

Method B. A mixture of $Fe(PEt_3)_2Cl_2$ (2.18 g, 6 mmol), $(Et_4N)_2[(Cl_4\text{-cat})MoOS_2FeCl_2]$ (**I**) (809 mg, 1.0 mmol) and $(Et_4N)_2[Fe_2S_2Cl_4]$ (**II**) (578 mg, 1.0 mmol) was dissolved in 30 mL of MeCN and stirred for 1 day. The reaction mixture was filtered with a fine porous frit, and the filtrate was kept for three weeks in the drybox. Rhombic-shaped black crystals (5 mg, 3.0 μmol, 0.9% yield based on Fe) were isolated.

X-ray Crystallography. Black rhombic-shaped crystals of $[(Cl_4\text{-cat})_2Mo_2Fe_6S_8(P^nBu_3)_6]$ (**IIIc**) were obtained from the slow diffusion of pentane into the dichloromethane solution and isolated by filtration. The transparent rhombic-shaped crystals of $(Et_4N)[Fe(PEt_3)Cl_3]$ (**VI**) were grown by slow diffusion of diethyl ether through the MeCN solution. Black rhombic crystals of $[(Cl_4\text{-cat})_2Mo_2Fe_2S_3O(PEt_3)_3Cl]\cdot 1/2(Fe(PEt_3)_2(MeCN)_4)$ (**VIII**) and $(Cl_4\text{-cat})_2Mo_2Fe_3S_5(PEt_3)_5$ (**X**) were obtained from saturated MeCN solution by standing in the drybox for a day and orange crystals of $(BPh_4)_2[Fe(PEt_3)_2(MeCN)_4]$ (**IX**) were obtained by slow evaporation of a MeCN solution. All diffraction data, except for **VIIa** and **VIIb**, were collected at 158(2) K using a Siemens SMART area diffractometer, data sets for **VIIa** and **VIIb** were collected at room temperature using a P3-F four circle diffractometer. The crystal data and structural parameters are shown in Tables 1 and 2. The structures for compounds **IIIc**, **V**, **VI**, **VIIa**, **VIIb**, **VIII**, **IX**, and **X** were solved by direct methods to locate heavy atoms, and the non-hydrogen atoms were located through subsequent difference Fourier syntheses. Structural refinement was carried out by full-matrix least-squares on F∧2. For the structure of **IIIc**, all the non-hydrogen atoms are refined anisotropically, except the severely disordered solvent molecule and C42. The monoclinic cell refinement for compound **V** produced no meaningful structure, and a triclinic cell was chosen. The O1 atom assignment in **VIII** gave the best thermal position parameters after trying S and N atoms. All non-hydrogen atoms were refined with anisotropic thermal parameters, and all hydrogen atoms were refined isotropically except those on disordered carbon atoms. Residual peaks of the disordered solvent molecule between two Cl_4-cat ligands in the structure of **X** were not refined further. All calculations were performed using SHELXTL-NT V. 5.1 software.

Results and Discussion

Synthesis. $(Et_4N)_2[(Cl_4\text{-cat})MoOFeS_2Cl_2]$ (I). Although the structure of **I** has been published, obtained as a decomposition product of the $[\{(Cl_4\text{-cat})MoFe_3S_4Cl_2\}_2(\mu\text{-S})(\mu\text{-NH}_2OH)]^{5-}$ cluster,[19] a detailed independent synthesis of **I** has not been reported as yet. The high yield synthesis of **I** is based on the reactivity of the Mo≡O group in the $[MoO_2S_2FeCl_2]^{2-}$ dimer.[29] The $[MoO_2S_2FeCl_2]^{2-}$ dimer is obtained easily and reproducibly as the Et_4N^+ salt from the reaction between $[Fe^{II}Cl_4]^{2-}$ and $[Mo^{VI}O_2S_2]^{2-}$ in MeCN. The Ph_4P^+ salt of the same anion was reported previously but was not characterized spectroscopically.[30] The reaction of one of the Mo≡O groups in $(Et_4N)_2[MoO_2S_2FeCl_2]$ with Cl_4-catH_2 produces dark green $(Et_4N)_2[(Cl_4\text{-cat})MoOS_2FeCl_2]$ (**I**) in MeCN with the Cl_4-cat ligand bound to the Mo atom. The reaction is accompanied by a color change from orange to dark green as soon as Cl_4-catH_2 is added. The electronic spectrum of compound **I** in MeCN shows absorptions at 630, 460, 360 nm, and these values are very similar to those published earlier.[19] The infrared spectrum of **I** in KBr shows vibrations associated with the Cl_4-cat and Mo≡O groups at 1437 and 939 cm^{-1}, respectively. The driving force for this reaction is formation of the Mo≡O group.[29] The ν(Mo≡O) shift from 902 and 877 cm^{-1} to 939 cm^{-1} shows the bond strength change from $(Et_4N)_2[MoO_2S_2FeCl_2]$ to compound **I** as the bond order of the Mo≡O group increases.

$(Cl_4\text{-cat})_2Mo_2Fe_6S_8(PR_3)_6$ [R = Et (IIIa), ^{n}Pr (IIIb), ^{n}Bu (IIIc)]. The synthesis of the $(Cl_4\text{-cat})_2Mo_2Fe_6S_8(PEt_3)_6$ cluster (**IIIa**) was originally reported in 1995,[15] and since then slight modifications have appeared.[31] The $NaBPh_4/PEt_3/(Et_4N)_2[(Cl_4\text{-cat})Mo(MeCN)Fe_3S_4Cl_3]$ (**VIIa**) reaction system employed in the reaction results in byproducts of NaCl, Et_4NBPh_4,[32] and

(29) Coucouvanis, D. *Adv. Inorg. Chem.* **1998**, *45*, 1.
(30) Schimanski, V. Thesis, University of Bielefeld, 1984.

Table 2. Crystal Data and Structure Refinements for $(Et_4N)_2[(Cl_4\text{-cat})Mo(THF)Fe_3S_4Cl_3]$ (**VIIb**), $[(Cl_4\text{-cat})_2Mo_2Fe_2S_3O(PEt_3)_3Cl]\cdot 1/2(Fe(PEt_3)_2(MeCN)_4)$ (**VIII**), $(BPh_4)_2[Fe(PEt_3)_2(MeCN)_4]$ (**IX**), and $(Cl_4\text{-cat})_2Mo_2Fe_3S_5(PEt_3)_5$ (**X**)

	VIIb	VIII	IX	X
empirical formula	$C_{26}H_{48}Cl_7Fe_3MoN_2O_3S_4$	$C_{44}H_{72}Cl_9Fe_{2.5}Mo_2N_4O_5P_4S_3$	$C_{68}H_{82}B_2FeN_4P_2$	$C_{42}H_{75}Cl_8Fe_3Mo_2O_4P_5S_5\cdot(C_2H_5O)$
formula weight	1148.65	1607.67	1094.79	1676.32
wavelength, Å	0.71073	0.71073	0.71073	0.71073
crystal system	monoclinic	monoclinic	triclinic	monoclinic
space group	*P*2(1)/*n*	*P*2(1)/*c*	*P*-1	*P*2(1)/*n*
unit cell dimensions, Å and deg	$a = 15.276(3)$	$a = 11.098(3)$	$a = 12.0756(10)$	$a = 14.811(3)$
	$b = 11.120(2)$	$b = 22.827(6)$	$b = 12.2070(10)$	$b = 22.188(4)$
	$c = 27.926(6)$	$c = 25.855(6)$	$c = 13.4024(11)$	$c = 21.864(4)$
			$\alpha = 93.2090(10)$	
	$\beta = 96.86(3)$	$\beta = 91.680(4)$	$\beta = 114.5760(10)$	$\beta = 100.124(3)$
			$\gamma = 116.6450(10)$	
volume, Å^3	4709.6(16)	6547(3)	1532.7(2)	7073(2)
Z, calcd density, mg/mm3	4, 1.620	4, 1.631	1, 1.186	4, 1.574
absorption coeff, mm^{-1}	1.775	1.519	0.342	1.547
F(000)	2340	3256	584	3416
crystal size, mm	0.10 × 0.10 × 0.60	0.32 × 0.32 × 0.20	0.38 × 0.24 × 0.20	0.38 × 0.22 × 0.20
θ range for data colln, deg	1.97−15.03	1.19−26.41	1.75−26.41	1.32−26.41
limiting indices	$0 < h < 11$	$-13 < h < 13$	$-13 < h <= 15$	$-18 < h < 18$
	$-8 < k < 8$	$-28 < k < 28$	$-15 < k < 15$	$-27 < k < 27$
	$-20 < l < 20$	$-32 < l < 32$	$-16 < l < 16$	$-27 < l < 27$
reflns collected/unique	3802/1894	62323/13425	15692/6225	67883/14510
R(int)	0.1151	0.0297	0.0253	0.0563
completeness to θ, %	98.8	99.8	99.0	99.8
data/restraints/parameters	1894/25/295	13425/0/731	6225/0/349	14510/0/667
goodness-of-fit on F^2	1.050	1.040	1.033	1.040
Final *R* indices [$I > 2\sigma(I)$]	R1 = 0.0809,	R1 = 0.0326,	R1 = 0.0388,	R1 = 0.0459,
	wR2 = 0.2193	wR2 = 0.0916	wR2 = 0.0943	wR2 = 0.1458
R indices (all data)	R1 = 0.1048,	R1 = 0.0430,	R1 = 0.0535,	R1 = 0.0580,
	wR2 = 0.2522	wR2 = 0.0970	wR2 = 0.0991	wR2 = 0.1547

$SPEt_3$. The isolation of $SPEt_3$ underscores the function of PEt_3 as a reducing agent. The $NaBPh_4$, $NaBF_4$, and $NaPF_6$ reagents supply Na^+ cations in organic solvent that remove Cl^- terminal ligands by precipitation as NaCl. A possible reaction scheme for the synthesis of **IIIa** can be envisioned, involving terminal ligand substitutions and reduction processes. The reaction using different phosphine ligands such as P^nPr_3 and P^nBu_3 produces the analogous products, $(Cl_4\text{-cat})_2Mo_2Fe_6S_8(P^nPr_3)_6$ (**IIIb**) and $(Cl_4\text{-cat})_2Mo_2Fe_6S_8(P^nBu_3)_6$ (**IIIc**).

The alternative use of $Fe(PR_3)_2Cl_2$ (R = Et, ^{n}Pr) in the synthesis of **IIIa** and **IIIb** also has been developed and results in slightly better yields. The isolation of $SPEt_3$ suggests a similar reaction pathway. Isolation of the new $(Et_4N)[Fe(PEt_3)Cl_3]$ compound (**VI**) as a byproduct in this reaction suggests that the latter forms from $Fe(PEt_3)_2Cl_2$ which serves as both a source of PEt_3 and a Cl^- scavenger (eqs 1−3).

$$Fe(PEt_3)_2Cl_2 \leftrightarrows Fe(PEt_3)Cl_2 + PEt_3 \text{ (new terminal ligand)} \quad (1)$$

$$Fe(PEt_3)Cl_2 + Cl^- \text{ (extracted terminal ligand)} \rightarrow [Fe(PEt_3)Cl_3]^- \quad (2)$$

$$[Fe(PEt_3)Cl_3]^- + (Et_4N)^+ \rightarrow (Et_4N)[Fe(PEt_3)Cl_3] \text{ (isolated byproduct)} \quad (3)$$

The important role of $(Cl_4\text{-cat})_2Mo_2Fe_6S_8(PR_3)_6$ (**III**) in nitrogenase synthetic analogue chemistry has been amplified recently not only because it has a core stoichiometry similar to the FeMoco but also because it can produce unprecedented Mo/Fe/S clusters[31,33] (Figure 3).

Although **III** is widely and extensively used as a valuable starting material, its synthesis has severe setbacks. Thus far, the synthesis of **III** has been achieved in low overall yield from the $(Et_4N)_2[(Cl_4\text{-cat})Mo(MeCN)Fe_3S_4Cl_3]$ cluster (**VIIa**). Even though the original synthesis of **VIIa** has been used for many years, it has not been improved and still is tedious and time-consuming. Cognizant of the importance of reductive coupling in the synthesis of Fe/S clusters, and the analogous versatile usage of the $Fe_2S_2(CO)_6$ building block in organometallic chemistry, we pursued the reductive coupling of the $(Et_4N)_2[(Cl_4\text{-cat})MoOFeS_2Cl_2]$ (**I**) and $(Et_4N)_2[Fe_2S_2Cl_4]$ (**II**) dimers for the direct synthesis of **III**.

The new synthetic approaches, using $NaPF_6/PR_3$ or $Fe(PR_3)_2Cl_2$ (R = Et, ^{n}Pr, and ^{n}Bu) as Cl^- removing reducing agents, with interdimer coupling of **I** and **II** afforded higher overall yields for $(Cl_4\text{-cat})_2Mo_2Fe_6S_8(P^nPr_3)_6$ (**IIIb**) (29% isolation yield) and $(Cl_4\text{-cat})_2Mo_2Fe_6S_8(PEt_3)_6$ (**IIIa**) (20% isolation yield) in considerably shorter reaction times. In the synthesis of **IIIa**, the $Fe_6S_6(PEt_3)_4Cl_2$ (**IV**) "basket" cluster is the major product. The presence of compound **IV**, which also forms during the original synthesis of **IIIa**, can be easily identified by ^{1}H NMR spectroscopy (characteristic chemical shift at −5.6 and −6.7 ppm in $CDCl_3$).[7] A similar reaction for the synthesis of $(Cl_4\text{-cat})_2Mo_2Fe_6S_8(P^nBu_3)_6$ (**IIIc**) produces a significant amount of this product but its high solubility prevents its isolation in yields better than 29%.

(31) (a) Osterloh, F.; Achim, C.; Holm, R. H. *Inorg. Chem*. **2001**, *40*, 224. (b) Osterloh, F.; Segal, B. M.; Achim. C.; Holm, R. H. *Inorg. Chem*. **2000**, *39*, 980. (c) Osterloh, F.; Sanakis, Y.; Staples, R. J.; Münck, E.; Holm, R. H. *Angew. Chem., Int. Ed*. **1999**, *38*, 2066.

(32) Transparent crystalline $(Et_4N)(BPh_4)$. FT-IR (KBr, cm^{-1}) 3054 (s), 3000 (m), 2984 (m), ν (C═C) 1942, 1987, and 1810, 1581 (m), 1480 (s), 744 (s), 735 (s), 707 (vs), 604 (s). Anal. Calcd for $BC_{32}H_{40}N$: C, 85.51; H, 8.97; N, 3.12. Found: C, 85.05; H, 8.97; N, 3.18.

(33) (a) Han, J.; Beck, K.; Ockwig, N.; Coucouvanis, D. *J. Am. Chem. Soc*. **1999**, *121*, 10448. (b) Tyson, M. A.; Coucouvanis, D. *Inorg. Chem*. **1997**, *36*, 3808.

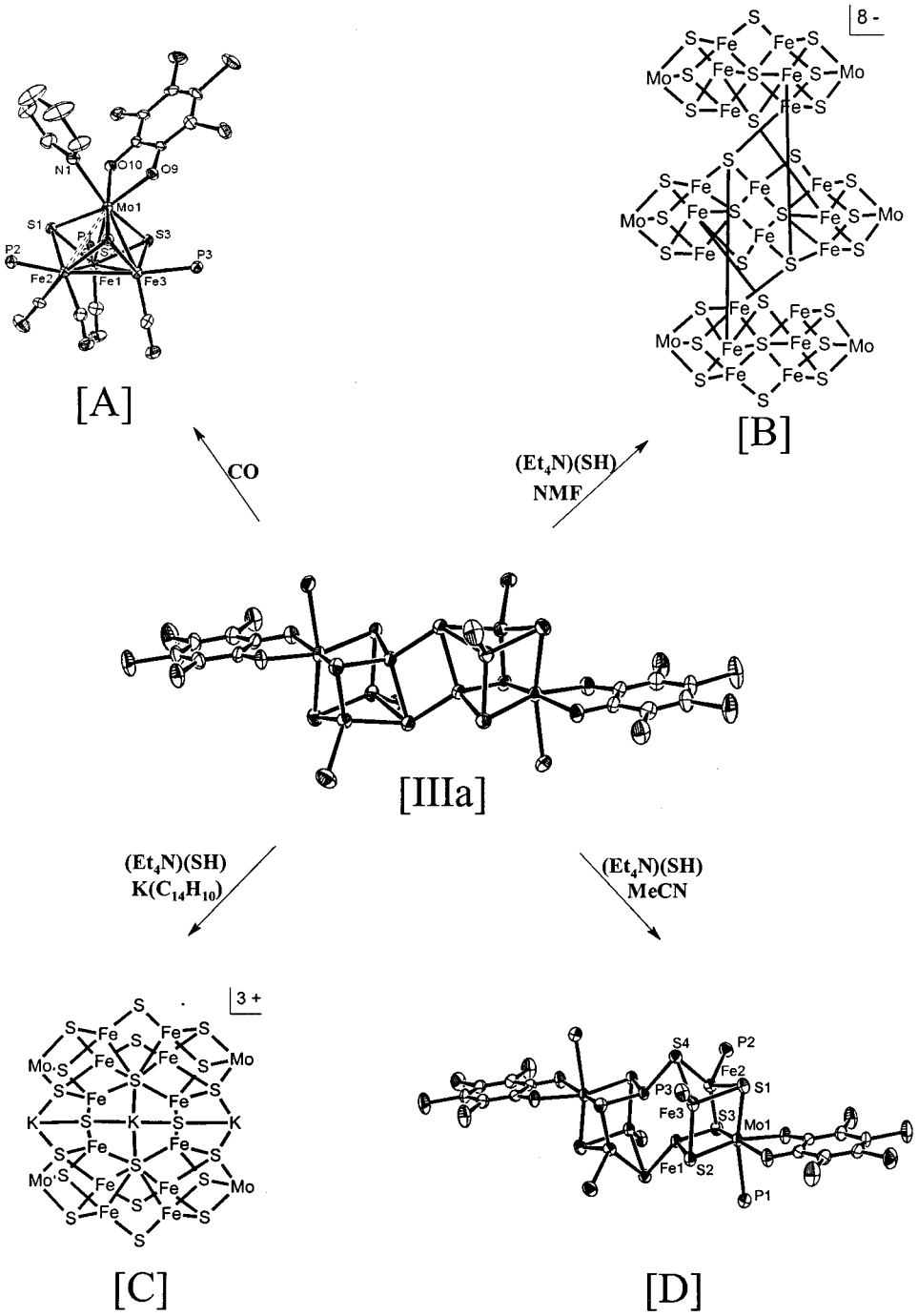

Figure 3. The Mo/Fe/S clusters synthesized from $(Cl_4\text{-cat})_2Mo_2Fe_6S_8(PEt_3)_6$ (**IIIa**). $(Cl_4\text{-cat})Mo(Pyr)Fe_3S_3(P^nPr_3)_3(CO)_4$ cluster **A** has been synthesized from $(Cl_4\text{-cat})_2Mo_2Fe_6S_8(P^nPr_3)_6$ (**IIIb**) by high-pressure CO reaction.[33] $[(Cl_4\text{-cat})_6Mo_6Fe_{20}S_{30}(PEt_3)_6]^{8-}$ (**B**),[31c] $[(Cl_4\text{-cat})_2Mo_4Fe_{12}S_{20}(PEt_3)_4K_3(DMF)]^{5-}$ (**C**),[31a] and $[(Cl_4\text{-cat})_2Mo_2Fe_6S_8(PEt_3)_6]^{4-}$ (**D**)[31a] have been synthesized from the reaction of $(Cl_4\text{-cat})_2Mo_2Fe_6S_8(PEt_3)_6$ (**IIIa**) with $(Et_4N)(SH)$ under different conditions.

A possible reaction pathway (Figure 4) may involve initial attack by trialkylphosphine on the Mo≡O group of compound **I** prior to or following chloride ligand substitution by PR_3. Formation of OPR_3 accompanies the two-electron reduction of compound **I**. Subsequently, the coupling of reduced **I** and **II** may proceed to form compound **III**. The selective extraction of the oxygen atom from $(Et_4N)_2[(Cl_4\text{-cat})MoOFeS_2Cl_2]$ cluster (**I**) by trialkylphosphine is evident by the nature of the products (compounds **III** and **VII**).

$Fe_6S_6(PEt_3)_4Cl_2$ (IV) and $(PF_6)[Fe_6S_8(P^nPr_3)_6]$ (V). The $Fe_6S_6(PEt_3)_4Cl_2$ (**IV**), "basket" cluster,[7] has been obtained by ligand substitution from the Fe/S clusters, $(^nBu_4N)_2[Fe_4S_4Cl_4]$ or $(Et_4N)_3[Fe_6S_6Cl_6]$, or by a self-assembly reaction using Li_2S/$FeCl_2$ in 60−70% yield. The isolation of **IV** as a byproduct in the synthesis of **IIIa** prompted us to examine the possible formation of **IV** from $(Et_4N)_2[Fe_2S_2Cl_4]$ (**II**) by a similar reaction. Not unexpectedly, **IV** was isolated from the reductive coupling of compound **II** in moderate yield (20−30%).

The formation of the hexanuclear $Fe_6S_6(PR_3)_4Cl_2$ (R = Et, ^{n}Bu) cluster, rather than $Fe_4S_4(PR_3)_3Cl$ or $[Fe_4S_4(PR_3)_4]^{+1}$ derivatives, has been rationalized by the effect of phosphine ligand cone angles.[34] Indeed, similar reaction with more bulky phosphine ligands, and larger cone angles than PEt_3 (132°),

(34) Tyson, M. A.; Demadis, K. D.; Coucouvanis, D. *Inorg. Chem.* **1995**, *34*, 4519.

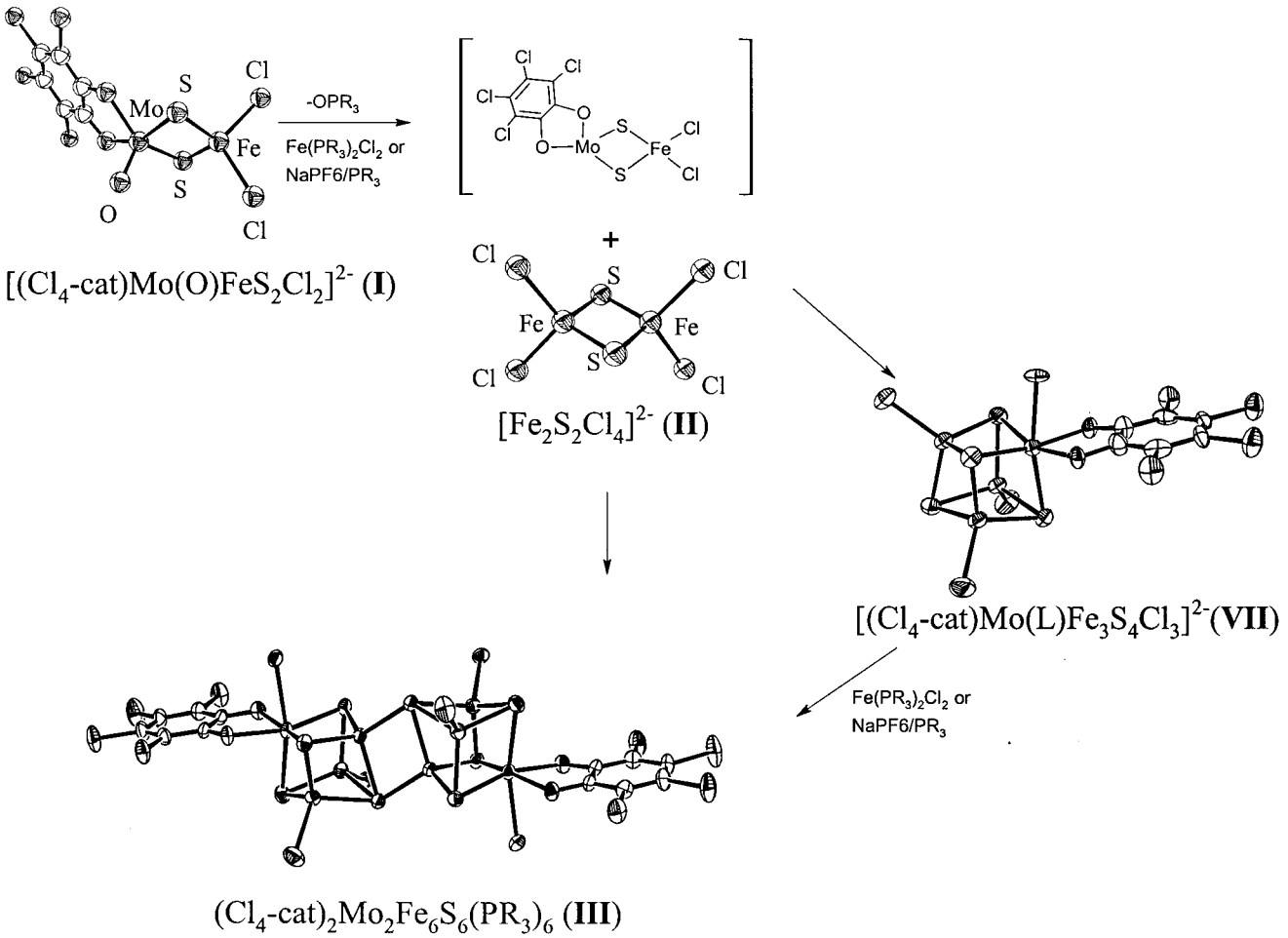

Figure 4. Possible reaction mechanism for the synthesis of $(Cl_4\text{-cat})_2Mo_2Fe_6S_8(PR_3)_6$ [R = Et (**IIIa**), ^{n}Pr (**IIIb**), ^{n}Bu (**IIIc**)] and $(Et_4N)_2[(Cl_4\text{-cat})Mo(L)Fe_3S_4Cl_3]$ [L = MeCN (**VIIa**), THF (**VIIb**)]. $(Et_4N)_2[(Cl_4\text{-cat})MoOFeS_2Cl_2]$ (**I**) reacts with PR_3 and results in the reduced intermediate, which undergoes reductive coupling with $(Et_4N)_2[Fe_2S_2Cl_4]$ (**II**). Depending on the ratio of chloride scavenger and PR_3, the coupling reaction produces **III** or **VII**. In the presence of excess reactants, compound **VII** may also form compound **III**.

produced $Fe_4S_4(PR_3)_3X$ and $Fe_4S_4(PR_3)_4X$ (R = ^{t}Bu, ^{i}Pr, and cyclopentyl, X = Cl, Br, and I).[34]

The original synthesis of the sulfido face-capped octahedral $[Fe_6S_8]^{2+}$ cluster has been achieved by the reaction of H_2S with $Fe(BF_4)_2{\cdot}H_2O$ and PEt_3 and obtained as a BF_4^- salt.[35] The clusters with different counteranions, BPh_4^- and PF_6^-, also have been prepared by simple anion exchange.[36] The multistep electron-transfer reactions of the $[Fe_6S_8]^{2+}$ cluster apparent in electrochemical measurements have made possible the isolation of these clusters in four different oxidation states.[37] Like other self-assembly reactions, the isolated yield of the $[Fe_6S_8]^{2+}$ cluster was relatively low (ca. 20%) and has not been improved yet. We have isolated cluster **V** as a byproduct in the synthesis of $(Cl_4\text{-cat})_2Mo_2Fe_6S_8(P^nPr_3)_6$ (**IIIb**). The reductive coupling of **II** to produce the P^nPr_3 analogue of **V** was attempted. When $(Et_4N)_2[Fe_2S_2Cl_4]$ (**II**) was reacted with 4 equiv of P^nPr_3 and $NaPF_6$ in MeCN, the reaction mixture produced the one electron reduced $[Fe_6S_8(P^nPr_3)_6]^+$ cluster isolated as a PF_6^- salt in 24% yield. The use of $(Bu_4N)_2[Fe_4S_4Cl_4]$ cluster, rather than **II**, produced crystalline **V** in higher yield (74%) under the same reaction conditions.

The reaction conditions for the synthesis of $Fe_6S_6(PEt_3)_4Cl_2$ (**IV**) and $(PF_6)[Fe_6S_8(P^nPr_3)_6]$ (**V**) are the same. In fact, Holm et al. reported the formation of the $[Fe_6S_6(PEt_3)_6]^+$ cluster under similar conditions.[38] Extra sulfur was added into their reaction system to support the $[Fe_6S_8(PEt_3)_6]^{2+}$ cluster. The formation of $(PF_6)[Fe_6S_8(P^nPr_3)_6]$ (**V**) cluster in our reaction system seems to be favored over the $Fe_6S_6(P^nPr_3)_4Cl_2$ cluster, although the $Fe_6S_6(PR_3)_4Cl_2$ [R = Et, ^{n}Bu], "basket" clusters have been isolated and the structure of $Fe_6S_6(P^nBu_3)_4Cl_2$ cluster reported.[7]

$(Et_4N)_2[(Cl_4\text{-cat})Mo(L)Fe_3S_4Cl_3]$ [L = MeCN (VIIa), THF (VIIb)]. The $[MoFe_3S_4]^{3+}$ cluster is a versatile starting material for the synthesis of other Mo/Fe/S clusters.[14,15,19,33,39] The cluster **VII** has been synthesized from $(Et_4N)_4[(Cl_4\text{-cat})_2Mo_2Fe_6S_8$-

(35) Cecconi, B.; Ghilardi, C. A.; Midollini, S. *J. C. S. Chem. Comm.* **1981**, 640.
(36) (a) Agresti, A.; Bacci, M.; Cecconi, F.; Ghilardi, C. A.; Midollini, S. *Inorg. Chem.* **1985**, *24*, 689. (b) Cecconi, F.; Ghilardi, C. A.; Midollini, S.; Orlandini, A.; Zanello, P. *J. Chem. Soc., Dalton Trans.* **1987**, 831. (c) Bencini, A.; Ghilardi, C. A.; Midollini, S.; Orlandini, A.; Russo, U.; Uytterhoeven, M. G.; Zanchini, C. *J. Chem. Soc., Dalton Trans.* **1995**, 963.
(37) Goddard, C. A.; Long, J. R.; Holm, R. H. *Inorg. Chem.* **1996**, *35*, 4347.
(38) Snyder, B. S.; Holm, R. H. *Inorg. Chem.* **1990**, *29*, 274.
(39) (a) Malinak, S. M.; Simeonov, A. M. Mosier, P. E.; McKenna, C. E.; Coucouvanis, D. *J. Am. Chem. Soc.* **1997**, *119*, 1662. (b) Demadis, K. D.; Malinak, S. M.; Coucouvanis, D. *Inorg. Chem.* **1996**, *35*, 4038. (c) Demadis, K. D.; Coucouvanis, D. *Inorg. Chem.* **1995**, *34*, 3658. (d) Demadis, K. D.; Coucouvanis, D. *Inorg. Chem.* **1995**, *34*, 436. (e) Demadis, K. D.; Chen, S. J.; Coucouvanis, D. *Polyhedron* **1994**, *13*, 3147. (f) Demadis, K. D.; Coucouvanis, D. *Inorg. Chem.* **1994**, *33*, 4195. (g) Coucouvanis, D.; Mosier, P. E.; Demadis, K. D.; Patton, S.; Malinak, S. M.; Tyson, M. A. *J. Am. Chem. Soc.* **1993**, *115*, 12193. (h) Coucouvanis, D.; Demadis, K. D.; Kim, C. G.; Dunham, R. W.; Kampf, J. W. *J. Am. Chem. Soc.* **1993**, *115*, 3344.

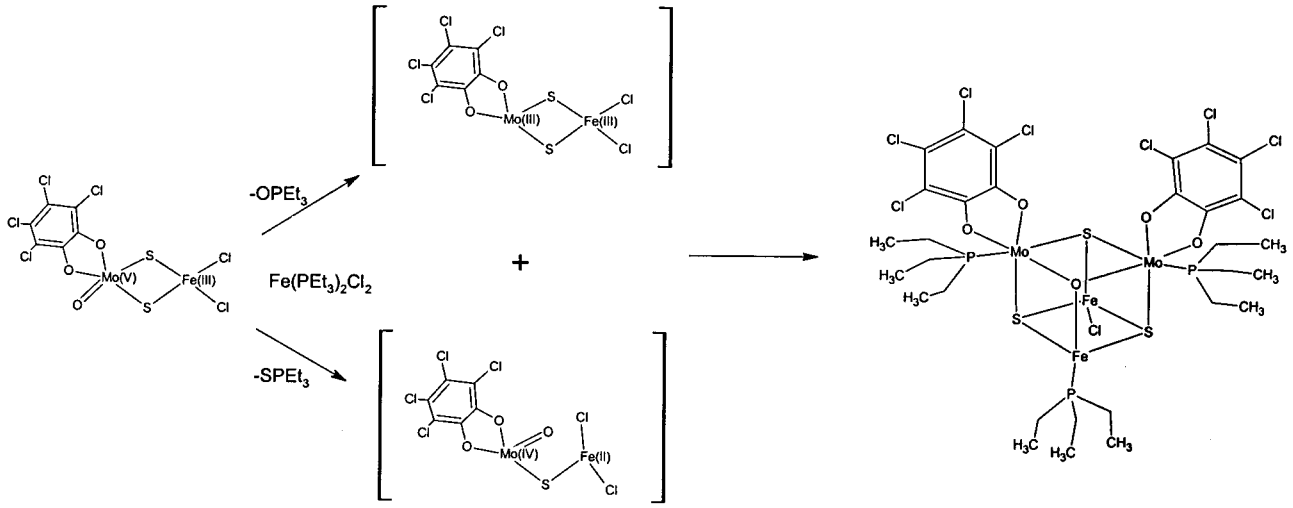

Figure 5. Proposed mechanism for the formation of the $[(Cl_4\text{-cat})_2Mo_2Fe_2S_3O(PEt_3)_3Cl]^-$ cluster (**VIII**). The reaction is driven by the oxidation of PEt_3, which gives $OPEt_3$ and $SPEt_3$, as the $2Mo^V$ and $2Fe^{III}$ are converted to Mo^{III}, Mo^{IV}, Fe^{II}, and Fe^{III}.

$(SEt)_6$] cluster after ligand exchange of SEt^- by Cl^- (by benzoyl chloride).[40] The $(Et_4N)_4[(Cl_4\text{-cat})_2Mo_2Fe_6S_8(SEt)_6]$ cluster is prepared from the $(Et_4N)_3[Mo_2Fe_7S_8(SEt)_{12}]$ cluster.[40(a)] The time-consuming process, involved in the original synthesis of **VII**, prompted us to seek a new synthetic route in the synthesis of this cluster (**VIIa**) bypassing the use of the octanuclear and nonanuclear precursors. This new route involves the reaction of equimolar amounts of **I**, **II**, and PEt_3 in the presence of slightly more than 2 equiv of $NaPF_6$. In the reaction, PEt_3 acts both as a ligand for the metal ions and a reducing, oxygen scavenger, from compound **I**. The $NaPF_6$ salt affords the Na^+ ions needed to remove Cl^- ligand from the reaction by precipitation of NaCl (Figure 4).

$[(Cl_4\text{-cat})_2Mo_2Fe_2S_3O(PEt_3)_3Cl]\cdot 1/2(Fe(PEt_3)_2(MeCN)_4)$ (VIII). Among the large number of cuboidal Mo/Fe/S clusters that have been reported,[41] clusters with the $[Mo_2Fe_2S_4]$ core are not very common, and those with the $[Mo_2Fe_2S_3O]$ core are unknown. Known clusters with the $[Mo_2Fe_2S_4]$ cores include (a) the $Mo_2Fe_2S_4(S_2CNEt_2)_5$ cluster obtained through a self-assembly reaction,[42] (b) the $Mo_2Fe_2S_4(pyrCS_2)_6$ cluster prepared from dinuclear complexes,[43] and (c) the structurally characterized organometallic clusters, $(Me_5C_5)_2Mo_2Fe_2S_4Cl_2$,[44] $Mo_2Fe_2S_4(C_5EtMe_4)_2(NO)_2$,[45] and $Mo_2Fe_2S_4(C_5Me_5)_2(CO)_4$.[46] These were obtained by condensation of $RMoX_n$ or $R_2Mo_2S_4X_n$ blocks (R = Cp or its derivatives, X = terminal ligand) and various iron sources ($FeCl_3$, $Na[Fe(CO)_3(NO)]$, $Fe_2(CO)_9$).

The reductive coupling of the $[(Cl_4\text{-cat})Mo(O)S_2FeCl_2]^{2-}$ dimer (**I**) in the absence of **II** was carried out with $Fe(PEt_3)_2Cl_2$ as a reducing and chloride scavenging agent and afforded the $(Cl_4\text{-cat})_2Mo_2Fe_2S_3O(PEt_3)_3Cl]\cdot 1/2(Fe(PEt_3)_2(MeCN)_4$ salt (**VIII**), with an anionic cluster containing the hitherto unknown $[Mo_2Fe_2S_3O]$ core. The formation of the new tetranuclear cluster (**VIII**) occurs by reduction of $(Et_4N)_2[(Cl_4\text{-cat})MoOS_2FeCl_2]$ with $Fe(PEt_3)_2Cl_2$ (eq 4).

$$4(Et_4N)_2[(Cl_4\text{-cat})Mo(O)S_2FeCl_2] + 10Fe(PEt_3)_2Cl_2 \rightarrow 2[(Cl_4\text{-cat})_2Mo_2Fe_2S_3O(PEt_3)_3Cl]^- + [Fe(PEt_3)_2(MeCN)_4]^{2+} + 2OPEt_3 + 2SPEt_3 + 8(Et_4N)(Fe(PEt_3)Cl_3) + FeCl_2(MeCN)_x \quad (4)$$

With the exception of $FeCl_2(MeCN)_x$, all other products shown in eq 4 have been isolated and characterized.

As stated previously, the versatility of the $Fe(PEt_3)_2Cl_2$ iron reagent has been demonstrated in the syntheses of the $(Cl_4\text{-cat})_2Mo_2Fe_6S_8(PR_3)_6$ [R = Et (**IIIa**), ^{n}Pr (**IIIb**)],[15,33a] and $Fe_6S_6(PEt_3)_4Cl_2$ (**IV**) clusters.[7] In the synthesis of **VIII**, the PEt_3 from $Fe(PEt_3)_2Cl_2$ abstracts S or O atoms from $(Et_4N)_2[(Cl_4\text{-cat})MoOS_2FeCl_2]$ with formation of $SPEt_3$ or $OPEt_3$ (Figure 5). Following reduction and ligand substitution (Cl^- by μ-S^{2-}), the Mo/Fe dimers undergo coupling and produce the $[Mo_2Fe_2S_3O]$ cuboidal cluster. The isolation of the $[Mo_2Fe_2S_3O]$ cluster but not of the $[Mo_2Fe_2S_4]$ or $[Mo_2Fe_2S_2O_2]$ clusters is perhaps fortuitous and intriguing. The $Fe(PEt_3)_2(MeCN)_4$ cation most likely forms from $Fe(PEt_3)_2Cl_2$ which is present in excess in the MeCN reaction mixture. To confirm the identity of the counterion in **VIII**, the $[BPh_4]^-$ complex of $Fe(PEt_3)_2(MeCN)_4$ (**IX**) was synthesized from $Fe(PEt_3)_2Cl_2$ and $NaBPh_4$ and identified (see Experimental Section).

The electronic spectrum of **VIII** shows a shoulder at 312 nm and an absorption band at 465 nm in MeCN solution. The $(Me_5C_5)_2Mo_2Fe_2S_4Cl_2$ cluster shows a multiabsorption electronic spectrum in THF solution with bands at 299, 459, 551, and 603 nm.[44] Cyclic voltammetry for compound **VIII** shows irreversible multielectron reduction waves at −882, −1140, and −1840 mV (vs SCE). A broad oxidation wave is also irreversible and appears at 412 mV. Oxidation of the cluster at higher potentials leads to decomposition. The electronic spectrum and cyclic voltammetric properties of **VIII** are similar to those observed for the "all-sulfido" $[Mo_2Fe_2S_4]$ clusters.[42−46]

$(Cl_4\text{-cat})_2Mo_2Fe_3S_5(PEt_3)_5$ (X). The reaction between $(Et_4N)_2[(Cl_4\text{-cat})(MeCN)MoFe_3S_4Cl_3]$ (**VIIa**) and $Fe(PEt_3)_2Cl_2$ pro-

(40) (a) Armstrong, W. H.; Holm, R. H. *J. Am. Chem. Soc.* **1981**, *103*, 6246. (b) Armstrong, W. H.; Mascharak, P. K.; Holm, R. H. *J. Am. Chem. Soc.* **1982**, *104*, 4373. (c) Palermo, R. E.; Singh, R.; Bashkin, J. K.; Holm, R. H. **1984**, *106*, 2600. (d) Palermo, R. E.; Holm, R. H. *J. Am. Chem. Soc.* **1983**, *105*, 4310.
(41) (a) Coucouvanis, D. *Acc. Chem. Res.* **1981**, *14*, 201. (b) Coucouvanis, D. *Acc. Chem. Res.* **1991**, *24*.1. (c) Holm, R. H. Simhon, E. D. In *Molybdenum Enzymes*; Spiro, T. G., Ed.; Wiley-Interscience: New York, 1985; pp 1−87.
(42) Xu, J.-Q.; Qian, J.-S.; Wei, Q.; Hu, N.-H.; Jin, Z.-S.; Wei, G.-C.; *Inorg. Chim. Acta*. **1989**, *164*, 55.
(43) Liu, Q.; Huang, L.; Lei, X.; Wang, F.; Chen, D.; Lu, J. *Sci. China. B.* **1991**, *34*, 1036.
(44) Kawaguchi, H.; Yamada, K.; Ohnish, S.; Tatsumi, K. *J. Am. Chem. Soc.* **1997**, *119*, 10871.
(45) Mansour, M. A.; Curtis, M. D.; Kampf, J. W. *Organometallics* **1997**, *16*, 275.
(46) Brunner, H.; Janietz, N.; Wachter, J.; Zahn, T.; Ziegler, M. *Angew. Chem., Int. Ed. Engl.* **1985**, *24*, 133.

duces the $(Cl_4\text{-cat})_2Mo_2Fe_6S_8(PEt_3)_6$ cluster (**IIIa**). The reaction also produces $Fe_6S_6(PEt_3)_4Cl_2$ cluster (**IV**) as a byproduct.[7] A minor product which can be isolated in the same reaction (see Experimental Section) is the $(Cl_4\text{-cat})_2Mo_2Fe_3S_5(PEt_3)_5$ cluster (**X**). The compound was crystallized from diethyl ether solution by slow solvent evaporation over several weeks under dinitrogen. The other synthetic route to **X** is associated with the reductive coupling of the $(Et_4N)_2[(Cl_4\text{-cat})MoOS_2FeCl_2]$ cluster (**I**). The coupling of **I**, in the presence or absence of **II** or inorganic S, produces **X** as a very minor product reproducibly.

The ^{1}H NMR spectrum of the $(Cl_4\text{-cat})_2Mo_2Fe_3S_5(PEt_3)_5$ cluster (**X**) was obtained in dichloromethane-d_2 at room temperature and showed an $S \neq 0$ spectrum with broadened resonances. Because of the complexity of the spectrum, only the methyl groups of the PEt_3 ligand could be assigned, based on the published NMR assignments for $(Cl_4\text{-cat})_2Mo_2Fe_6S_8(PEt_3)_6$[31b] and $Fe_6S_6(PEt_3)_4Cl_2$.[7,38] The methyl group resonances of the three PEt_3 ligands on the Fe atoms are found at 0.89 and 0.08 ppm in a 1 to 2 ratio. The other methyl group resonances of the PEt_3 ligands coordinated to the Mo atoms are found at 1.27 and 1.16 ppm. The ^{1}H NMR spectrum shows a characteristic peak at $-$ 2.02 ppm that was assigned to one of the methylene groups of the PEt_3 bound to the Fe atoms. The NMR spectrum is consistent with a cluster that has two electronically equivalent Fe types with two equivalent Fe atoms in one, and one unique Fe atom in the other. Two different Mo centers also are evident.

The $(Cl_4\text{-cat})_2Mo_2Fe_3S_5(PEt_3)_5$ cluster shows irreversible poorly defined, multistep cyclic voltammetric waves in 1,2-dichloroethane with 0.1 M of $^nBu_4NPF_6$ as supporting electrolyte vs SCE reference electrode. The compound shows three successive irreversible reduction potentials from $-$480 to $-$1140 mV with separations of about 300 mV. A multielectron oxidation at 650mV also was observed. The overall cyclic voltammogram of **X** is very similar to those of the $(Cl_4\text{-cat})Mo(L)Fe_3S_3(CO)_6(PR_3)_2$ [L = O, Pyr, or P^nPr_3, R = Et or ^{n}PR] compounds.[47]

Structural Description. $(Cl_4\text{-cat})_2Mo_2Fe_6S_8(PR_3)_6$ [R = Et (IIIa), ^{n}Pr (IIIb), ^{n}Bu (IIIc)].[48] The $(Cl_4\text{-cat})_2Mo_2Fe_6S_8(PR_3)_6$ clusters with PEt_3, P^nPr_3, or P^nBu_3 ligand have been characterized structurally by single-crystal X-ray crystallography. The crystallographic structure of **IIIa** in the monoclinic $P2_1/c$[15] or the triclinic P-1[31b] system has been reported before and discussed briefly. **IIIb** crystallizes in the orthorhombic system with a = 19.3626(3) Å, b = 17.47610(10) Å, c = 17.9367(3) Å. Satisfactory structural refinement of the data was not possible because the crystal is extremely sensitive to solvent loss. Partial refinement of the structure (R1 = 18.96 for all data) assigned all the heavy atoms in the core as well as the P and O atoms coordinated to the metal atoms. The synthesis of **IIIc** has been reported before without structural data.[15] The crystallographic structure of **IIIc** is reported here, and its structure is almost identical to **IIIa** as shown in Figure 6.

The $(Cl_4\text{-cat})_2Mo_2Fe_6S_8(PR_3)_6$ [R = Et (**IIIa**), ^{n}Pr (**IIIb**), ^{n}Bu (**IIIc**)] cluster shows two edge-sharing $[MoFe_3S_4]$-"cubane" units that define an octanuclear cluster. The same bridging pattern was later found in the $Fe_8S_8(PCy_3)_6$8 and $[Fe_8S_8(2,4,6\text{-}Me_3C_6H_2NC)_{18}][B(4\text{-}ClPh)_4]_2$ clusters.[49] The bridge between the two $[MoFe_3S_4]^{2+}$ units in **IIIa** and **IIIc** defines a $[Fe_2S_2]$ rhomb which has short Fe$-$Fe distances of 2.659(15) and 2.6512(17) Å for **IIIa** and **IIIc**, respectively. The short, bridging, Fe$-$Fe bond distances are still longer than the M$-$M distances throughout the $[Mo_2Fe_6S_8]^{4+}$ core. The average intracubane Fe$-$Fe distances of **IIIa** and **IIIc** are 2.639(3) Å (range: Fe$-$Fe, 2.632(2)$-$2.649(3) Å) and 2.622(5) Å (range: Fe$-$Fe, 2.6127(13)$-$2.6302(13) Å), respectively. The bridging Fe$-$Fe distances in $Fe_8S_8(PCy_3)_6$[8] and $[Fe_8S_8(2,4,6\text{-}Me_3C_6H_2NC)_{18}]^{+}$[49] are found at 2.681(8) and 2.766(4) Å, respectively.

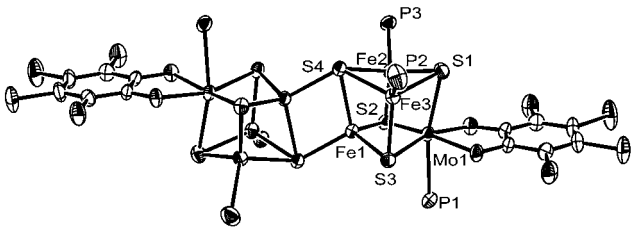

Figure 6. Single-crystal X-ray structure of $(Cl_4\text{-cat})_2Mo_2Fe_6S_8(P^nBu_3)_6$ clusters (**IIIc**). The *n*-butyl groups of tri-*n*-butylphosphine were omitted, and tetrachlorocatecholate ligands were simplified for clarity. Selected distances [Å] and angles [deg]: Mo1$-$Fe1, 2.6815(10); Mo1$-$Fe2, 2.6479(11); Mo1$-$Fe3, 2.6658(11); Fe1$-$Fe2, 2.6127(13); Fe2$-$Fe3, 2.6230(13); Fe1$-$Fe3, 2.6302(13); S4$-$Fe1$-$S4#1, 110.82(6); Fe1$-$S4$-$Fe1#1, 69.17(6).

The Mo(1)$-$Mo(1) distances are found at 7.864(2) and 7.849(2) Å in **IIIa** and **IIIc**. The average Mo$-$Fe distance in **IIIa** is found at 2.677(5) Å (range: 2.658(2)$-$2.695(2) Å) and that in **IIIc** is found at 2.665(10) Å (range: 2.6479(11)$-$2.6815(10) Å), respectively. A slight longitudinal contraction of the MoFe cores is found for **IIIc** by comparison to **IIIa** and is reflected in the Mo$-$Mo and Mo$-$Fe distances. This is probably due to small differences in the σ-donating/π-accepting property of the trialkylphosphine ligand.[50] The phosphine ligand with longer alkyl chains can donate more electron density to the metal. This seems to strengthen (and shorten) the M$-$M bonding by increasing electron density in M$-$M bonding orbitals. A comparison of the metal$-$phosphine bonds between **IIIa** and **IIIc** shows the Mo atom to be more sensitive to phophine ligand changes. The Mo atoms in **IIIa** shows octahedral coordination geometry and an average Mo$-$P distance of 2.601(4) Å. The corresponding bond in **IIIc** is found at 2.5748(19) Å. The average Fe$-$P distances in **IIIa** and **IIIc** show no significant difference and are found at 2.336(7) and 2.343(11) Å, respectively.

$(PF_6)[Fe_6S_8(P^nPr_3)_6]$ (V). The sulfur face-capped octahedral $[Fe_6S_8(PEt_3)_6]^{n+}$ cluster and its derivatives ($n = 0-3$) have been characterized structurally and discussed before.[37] Since the $(PF_6)[Fe_6S_8(P^nPr_3)_6]$ cluster (**V**) is the only non-PEt_3 ligated $[Fe_6S_8(PR_3)_6]^+$ cluster (Figure 7), its structure has been compared to the corresponding $(PF_6)[Fe_6S_8(PEt_3)_6]$ cluster.[36(b)] The Fe$-$Fe distances in **V** are found in the range of 2.5988(7) to 2.6050(7) Å with an average value of 2.6019(12) Å. This value is significantly shorter than that in the $(PF_6)[Fe_6S_8(PEt_3)_6]$ cluster (2.636(2) Å) and even shorter than that of the one-electron oxidized $(PF_6)_2[Fe_6S_8(PEt_3)_6]$ cluster (2.617(6) Å).[36b] The shorter Fe$-$Fe bonds in **V** have resulted in the elongation of the Fe$-$S bonds. The Fe$-$S distances are found in the range of 2.2682(11) to 2.2844(8) Å with an average value is 2.273(2) Å. The average Fe$-$S distance of $(PF_6)[Fe_6S_8(PEt_3)_6]$ cluster is found at 2.251(3) Å. The average Fe$-$S$-$Fe angle in **V** at 69.83(7)° is more acute than that in the $(PF_6)[Fe_6S_8(PEt_3)_6]$ cluster at 71.7(1)°. The

(47) Coucouvanis, D.; Han, J.; Moon, N. *J. Am. Chem. Soc.*, submitted.
(48) Comprehensive structural description of **IIIa** are found in Kostas, D. Thesis, University of Michigan, 1995.
(49) Harmjanz, M.; Saak, W.; Haase, D.; Pohl, S. *Chem. Commun*. **1997**, 951.
(50) (a) Alyea, E. C.; Song, S. *Comments Inorg. Chem*. **1996**, *18*, 189. (b) Rhaman, Md. M.; Liu, H. Y.; Prock, A.; Giering, W. P. *Organometallics* **1987**, *6*, 650.

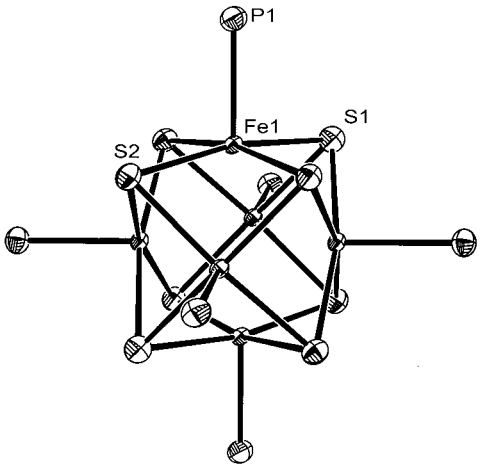

Figure 7. Single-crystal X-ray structure of $[Fe_6S_8(PEt_3)_6]^+$ cluster (**V**). The *n*-propyl group of P^nPr_3 was omitted for clarity. Selected distances [Å] and angles [deg]: Fe1−Fe1#1, 2.6050(7); Fe1−Fe1#2, 2.6050(7); Fe1−Fe1#3, 2.5988(7); Fe1−Fe1#4, 2.5988(7); Fe1−S1, 2.2716(8); Fe1−S1#1, 2.2702(8); Fe1−S1#2, 2.2844(8); Fe1−S2, 2.2682(11); Fe1#1−S1, 2.2844(8); Fe1#2−S1, 2.2702(8); Fe1#3−S2, 2.2682(11); Fe1#4−S2, 2.2682(11); Fe1−P1, 2.3169(9); Fe1#3−Fe1−Fe1#1, 90; Fe1#4−Fe1−Fe1#2, 90; Fe1#3−Fe1−Fe1#4, 60; Fe1#3−Fe1−Fe1#2, 60.078(10); Fe1#4−Fe1−Fe1#1, 60.078(10); Fe1#2−Fe1−Fe1#1, 59.84(2); S2−Fe1−S1, 167.95(3); S2−Fe1−S1#1, 89.79(2); S1#1−Fe1−S1, 89.28(2); S2−Fe1−S1#2, 89.43(2); S1#1−Fe1−S1#2, 167.68(3); S1−Fe1−S1#2, 88.92(2); Fe1−S1−Fe1#2, 70.00(3); Fe1#1−S1−Fe1#2, 69.58(3); Fe1−S1−Fe1#1, 69.75(3); Fe1−S2−Fe1#3, 69.90(4); Fe1−S2−Fe1#4, 69.90(4); Fe1#3−S2−Fe1#4, 69.90(4). Symmetry transformations used to generate equivalent atoms: #1, $y-1, -x+y, -z$; #2, $x-y+1, x+1, -z$; #3, $-y+1, x-y+2, z$; #4, $-x+y-1, -x+1, z$.

overall structure of **V** is similar to that of the $[Fe_6S_8(PEt_3)_6]^+$ cluster with all Fe atoms slightly compressed toward the center of the core structure. The general slight decrease of the M−M distances upon increase of the PR_3 ligand alkyl chain length, observed in the structures of **IIIa** and **IIIc**, also is observed in the structure of **V**.

The $(Et_4N)[Fe(PEt_3)Cl_3]$ monomer (**VI**) is the one phosphine-substituted analogue of $(Et_4N)_2[FeCl_4]$.[51] The average Fe−Cl bond distance in $(Me_4N)_2[FeCl_4]$ at 2.292(2) Å[52] is a little shorter than that in **VI** at 2.282(4) Å. The Fe−P bond in **VI** at 2.439(4) Å is longer than the average Fe−P distance in **IIIa** at 2.336(7) Å. The tetrahedrally coordinated Fe atom in compound **VI** shows an average Cl−Fe−Cl angle of about 112.3(6)°.

$(Et_4N)_2[(Cl_4\text{-cat})Mo(L)Fe_3S_4Cl_3]$ [L = MeCN (VIIa), THF (VIIb)]. Although numerous clusters with $[MoFe_3S_4]^{3+}$ core have been synthesized and their structures have been reported,[12,14,39] the structures of **VIIa** and **VIIb** have not been reported as yet. Since they are important precursors for other Mo/Fe/S clusters, we compared the structures of **VIIa** and **VIIb** (Figure 8) with other known $(Et_4N)_2[(Cl_4\text{-cat})Mo(L)Fe_3S_4Cl_3]$ (L = $MeNHNH_2$, $MeNH_2$) and $(Et_4N)_3[(Cl_4\text{-cat})Mo(Cl)Fe_3S_4Cl_3]$ clusters.[14] As shown in Table 3, the overall structure of the core in the $[MoFe_3S_4]^{3+}$ clusters does not change significantly. The average Mo−Fe distances are found in the range of 2.729(11) to 2.754(5) Å and those of Fe−Fe distances are found in the range of 2.709(19) to 2.733(5) Å. The average Mo−S and Fe−S distances are found in the range of 2.353(9) to 2.37(1) Å and in the range of 2.268(11) to 2.275(8) Å respectively. The average Fe−Fe distances in the $[MoFe_3S_4]^{2+}$ cores of **IIIa** and **IIIc** are at 2.639(3) and 2.622(5) Å, respectively. Hence the one-electron reduction of the $[MoFe_3S_4]^{3+}$ cluster appears to shorten the Fe−Fe bond distances of the cluster. The average Fe−Cl distances of the compounds in Table 3 are found in the range of 2.207(16) to 2.236(9) Å. The values are shorter than that found in **IV** (2.282(4) Å).

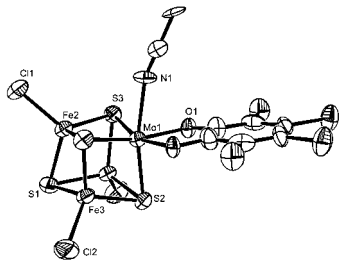

VIIa

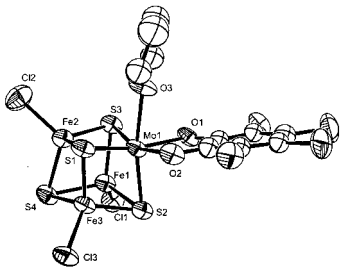

VIIb

Figure 8. Single-crystal X-ray structure of $(Et_4N)_2[(Cl_4\text{-cat})Mo(L)Fe_3S_4Cl_3]$ [L = MeCN (**VIIa**), THF (**VIIb**)] clusters. The countercation, $(Et_4N)^+$, and hydrogen atoms were omitted for clarity.

Table 3. The Average Bond Distance Comparison of $(Et_4N)_2[(Cl_4\text{-cat})Mo(L)Fe_3S_4Cl_3]$ [L = MeCN (V**IIa**), THF (V**IIb**), $MeNHNH_2$, $MeNH_2$, and $(Et_4N)_3[(Cl_4\text{-cat})MoFe_3S_4Cl_4]$ Clusters[14]

ligand on Mo	MeCN (**VIIa**)	THF (**VIIb**)	$MeNHNH_2$[a]	$MeNH_2$[a]	Cl^-[a]
Mo−O	2.052(12)	2.09(3)	2.11(3)	2.09(2)	2.102(19)
Mo-L	2.29(3)	2.295(17)	2.27(3)	2.28(2)	2.538(10)
Mo−S	2.354(9)	2.341(9)	2.367(10)	2.353(9)	2.343(11)
Mo−Fe	2.754(5)	2.742(6)	2.729(11)	2.735(9)	2.749(10)
Fe−S	2.275(8)	2.269(10)	2.273(10)	2.268(11)	2.272(11)
Fe−Fe	2.733(5)	2.716(7)	2.722(10)	2.724(14)	2.707(19)
Fe−Cl	2.221(16)	2.207(16)	2.22(2)	2.215(11)	2.222(13)

[a] Reference 14.

$[(Cl_4\text{-cat})_2Mo_2Fe_2S_3O(PEt_3)_3Cl]\bullet 1/2(Fe(PEt_3)_2(MeCN)_4)$ (VIII). In the structure of **VIII**, the $(Cl_4\text{-cat})_2Mo_2Fe_2S_3O(PEt_3)_3$-Cl anions are located on either side of the *trans*-$[Fe(PEt_3)_2(MeCN)_4]^{2+}$ dication which is situated on a crystallographic center of symmetry. Two molecules of MeCN are found for each $(Cl_4\text{-cat})_2Mo_2Fe_2S_3O(PEt_3)_3Cl$ anion. The monoanionic tetranuclear cluster consists of two interpenetrating Mo_2Fe_2 and S_3O tetrahedra (Figure 9). The overall structural features of the $[Mo_2Fe_2S_3O]^{4+}$ core in **VIII** are similar to those found in the $[Mo_2Fe_2S_4]$ distorted cubanes except that the μ_3-O atom is positioned lower above the Mo(1)−Mo(2)−Fe(2) plane at 1.304(2) Å. In contrast, the μ_3-S(3) atom is positioned at 1.728(1) Å above the Mo1−Mo2−Fe1 plane. This difference is a direct consequence of the Mo−O and Fe−O bonds. These bonds at 2.035(2), 2.037(2), and 1.910(2) Å for Mo(1)−O(1), Mo(2)−O(1), and Fe(2)−O(1), respectively, are considerably shorter than the M−S(3) bonds (Mo(1)−S(3), 2.3693(9) Å; Mo(2)−S(3), 2.3590(9) Å; Fe(2)−S(3), 2.2595(10) Å). The dihedral angle between the Mo(1)−Mo(2)−Fe(2) and Mo(1)−Mo(2)−Fe(1) planes is 71.42(2)°. The Mo−O(1) distances in

(51) Due to extreme air-sensitivity of the compound, the structure solution better than R1 = 0.1415 was not possible.

(52) Lauher, J. W.; Ibers, J. A. *Inorg. Chem.* **1975**, *2*, 348.

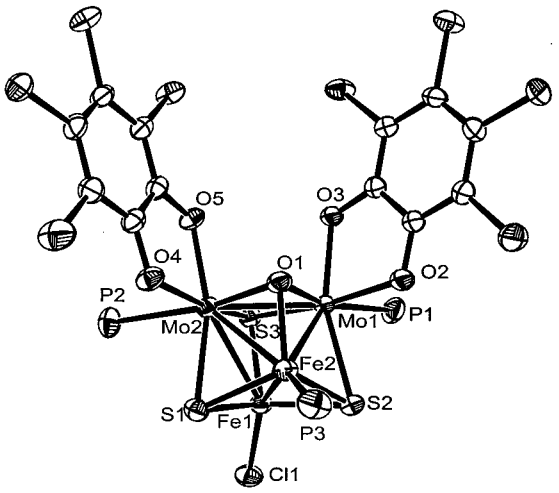

Figure 9. Single-crystal X-ray structure of $[(Cl_4\text{-cat})_2Mo_2Fe_2S_3O(PEt_3)_3\text{-}Cl]^-$ anion (**VIII**). The ethyl groups of triethylphosphine were omitted for clarity. The carbon atoms and chloride atoms were not labeled. Selected distances [Å] and angles [deg]: Mo1−Mo2, 2.6602(6); Mo1−Fe1, 2.7260(7); Mo1−Fe2, 2.5695(7); Mo2−Fe1, 2.7071(8); Mo2−Fe2, 2.6001(7); Fe1−Fe2, 2.6792(9); Mo1−O1, 2.035(2); Mo1−S2, 2.3593(10); Mo1−S3, 2.3693(9); Mo1−P1, 2.5846(11); Mo1−O2, 2.100(2); Mo1−O3, 2.064(2); Mo2−O1, 2.037(2); Mo2−S1, 2.3678(10); Mo2−S3, 2.3590(9); Mo2−P2, 2.5857(11); Mo2−O4, 2.100(2); Mo2−O5, 2.080(2); Fe1−S1, 2.2714(10); Fe1−S2, 2.2657(10); Fe1−S3, 2.2595(10); Fe1−Cl1, 2.2212(10); Fe2−O1, 1.910(2); Fe2−S1, 2.2326(10); Fe2−S2, 2.2393(10); Fe2−P3, 2.3648(12); O1−Mo1−S3, 88.09(9); O1−Mo1−S2, 100.04(7); S2−Mo1−S3, 101.64(3); O1−Mo2−S3, 104.40(7); O1−Mo2−S1, 168.06(7); S1−Mo2−S3, 102.90(3); S1−Fe1−S2, 100.91(4); S1−Fe1−S3, 109.35(4); S2−Fe1−S3, 108.19(4); Cl1−Fe1−S1, 112.15(4); Cl1−Fe1−S2, 113.47(4); Cll−Fe1−S3, 112.14(4); S1−Fe2−S2, 102.96(4); O1−Fe2−S1, 107.24(8); O1−Fe2−S2, 108.55(8).

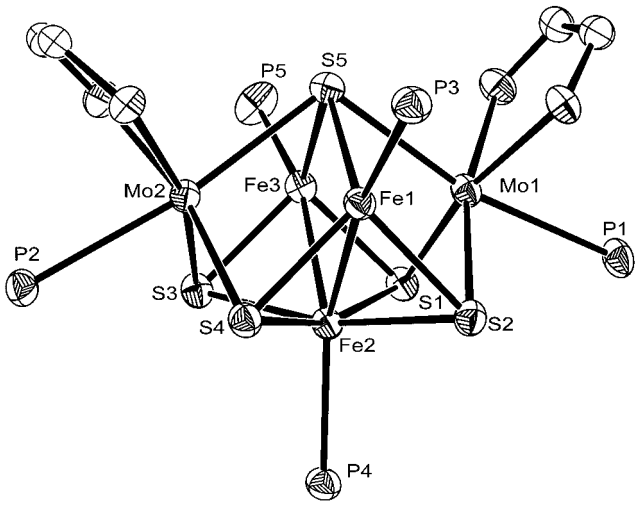

Figure 10. Single-crystal X-ray structure of $(Cl_4\text{-cat})_2Mo_2Fe_3S_5(PEt_3)_5$ (**X**). The ethyl groups of triethylphosphine were omitted, and tetrachlorocatecholate ligands were simplified for clarity.

VIII are similar to those observed for other compounds with the Mo-μ_3-O unit.[53] The Fe−O(1) distances in **VIII** are found within the typical range of 1.82∼1.97 Å for Fe(III)−(μ_3-O).[54] The fact that Fe(III)−(μ_2-OH) distances are usually found at distances longer than 1.93 Å ensure that O(1) is not a hydroxyl ligand.[55] In fact, $(C_5Me_5)_2Mo_2Fe(CO)_7(\mu_3\text{-O})$, the only known compound with the $Mo_2Fe(\mu_3\text{-O})$ moiety has very similar bond lengths.[56] In the latter, the Mo−O bonds are 2.015(3) and 2.019(3) Å and the Fe−O bond is found at 1.902(3) Å.

As a result of the short M−O bonds, short M−M distances are apparent in **VIII**. These at 2.5695(7) and 2.6001(7) Å for Mo(1)−Fe(2) and Mo(2)−Fe(2) are much shorter than those at 2.7260(7) and 2.7071(8) Å found for Mo(1)−Fe(1) and Mo(2)−Fe(1). The short Mo(1)−Mo(2) distance of 2.6602(6) Å is also a consequence of the short Mo−O bonds. The short Fe(1)−Fe(2) distance at 2.6792(9) Å may imply metal−metal interactions. The Fe−Fe distance in $(Et_4N)_2[Fe_2S_2Cl_4]$ (**II**) is 2.716(1) Å and those in $(^nBu_4N)_2[Fe_4S_4Cl_4]$ are 2.755(2) and 2.766(4) Å. The Fe−Fe distance of $(Et_4N)_2[(Cl_4\text{-cat})(MeCN)MoFe_3S_4\text{-}Cl_3]$ is 2.733(5) Å and that in $Mo_2Fe_2S_4(S_2CNEt_2)_5$ cluster is found at 2.784(3) Å. The Fe(1)−Fe(2) distance in **VIII** is the shortest among similar clusters and much shorter (∼0.1 Å) than that in the related $Mo_2Fe_2S_4(S_2CNEt_2)_5$ cluster.

The $[Fe(PEt_3)_2(MeCN)_4]^{2+}$ dication is analogous to the known $[Fe(Ph_2PCH_2)_2(MeCN)_4]^{2+}$.[57] The trans arrangement of the PEt_3 ligands in these complexes also has been observed in the structures of six-coordinate pseudo-octahedral porphyrin complexes that contain the FeP_2N_4 core.[58] The centrosymmetric $[Fe(PEt_3)_2(MeCN)_4]^{2+}$ monomer can be synthesized independently as a BPh_4^- salt. The spectroscopic characteristics of this cation are identical to those of the cation in **VIII**.

In the structure of $(BPh_4)_2[Fe(PEt_3)_2(MeCN)_4]$ (**IX**), the six coordinate cation is situated on a crystallographic center of symmetry and has a pseudo-octahedral coordination geometry. The Fe(3)−P(4) distance is 2.3103(10) Å and those of Fe(3)−N(1) and Fe(3)−N(2) are 1.917(3) and 1.915(3) Å, respectively. The same bonds in **VIII** show almost the same distances (Fe−P; 2.3131(5) Å and Fe−N; 1.940(15) and 1.920(15) Å). The *trans*-porphyrinato-Fe(II)-bis(phosphine) complexes show Fe−P distances between 2.2750(6) and 2.346(1) Å depending on the phosphine ligands used. The Fe−N distances for the same complexes are in the range from 1.991(2) to 1.999(2) Å. The Fe−P and Fe−N distances in the $[Fe(Ph_2PCH_2)_2(MeCN)_4]^{2+}$ monomer, which has the PR_3 ligands in a *cis*-configuration, are 2.251(6) and 1.950(13) Å, respectively.[57]

$[(Cl_4\text{-cat})_2Mo_2Fe_3S_5(PEt_3)_5]$ (X). The structure of $(Cl_4\text{-cat})_2\text{-}Mo_2Fe_3S_5(PEt_3)_5$ (**X**) cluster can be described as a square pyramidal Mo_2Fe_3 metal cluster with each of the faces (four triangular and one square) bridged by sulfide ligands (four μ_3 and one μ_4) (Figure 10). The arrangement of the sulfide ligands

(53) Song, L.-C.; Fan, H.-T.; Hu, Q.-M.; Qin, X.-D.; Zhu, W.-F.; Chen, Y.; Sun, J. *Organometallics* **1998**, *17*, 3454.

(54) (a) Armstrong, W. H.; Roth, M. E.; Lippard, S. J. *J. Am. Chem. Soc.* **1987**, *109*, 6318. (b) Caneschi, A.; Cornia, A.; Fabretti, A. C.; Gatteschi, D. *Angew. Chem., Int., Ed. Engl.* **1995**, *34*, 2716. (c) Poliakova, L. A.; Gubin, S. P.; Belyakova, O. A.; Zubavichus, Y. V.; Slovokhotov, Y. L. *Organometallics* **1997**, *16*, 4527. (d) Hegetschweiler, K.; Hausherr-Primo, L.; Koppenol, W. H.; Gramlich, V.; Odier, L.; Meyer, W.; Winkler, H.; Trautwein, A. X. *Angew. Chem., Int. Ed. Engl.* **1995**, *34*, 2242.

(55) (a) Ou, C. C.; Lalancette, R. A.; Potenza, J. A.; Schugar, H. J. *J. Am. Chem. Soc.* **1978**, *100*, 2053. (b) Harvey, D. F.; Christmas, C. A.; McCusker, J. K.; Hagen, P. M.; Chadha, R. K.; Hendrickson, D. N. *Angew. Chem., Int., Ed. Engl.* **1991**, 30, 598. (c) Hogarth, G.; Lavender, M. H. *J. Chem. Soc., Dalton Trans.* **1993**, 143.

(56) Gibson, C. P.; Huang, J.-S.; Dahl, L. F. *Organometallics* **1986**, *5*, 1676.

(57) Pohl, S.; Opitz, U. *Angew. Chem., Int. Ed. Engl.* **1993**, *32*, 863.

(58) (a) Sodano, P.; Simonneaux, G.; Toupet, L. *J. Chem. Soc., Dalton. Trans.* **1988**, 2615. (b) Belani, R. N.; James, B. R.; Dolphin, D.; Rettig, S. J. *Can. J. Chem.* **1988**, *66*, 2072. (c) Toupet, L.; Sodano, P.; Simonneaux, G. *Acta Crystallogr., Sect. C.* **1990**, *46*, 1631. (d) Toupet, L.; Legrand, N.; Bondon, A.; Simonneaux, G. *Ibid.* **1994**, *50*, 1014. (e) Pilard, M.-A.; Guillemot, M.; Toupet, L.; Jordanov, J.; Simonneaux, G. *Inorg. Chem.* **1997**, *36*, 6307. (f) Mink, L. M.; Polam, J. R.; Christensen, K. A.; Bruck, M. A.; Walker, F. A. *J. Am. Chem. Soc.* **1995**, *117*, 9329.

also is square pyramidal. The total number of valence electrons in **X** at 70 is four electrons fewer than the number expected for a completely bonded square pyramidal cluster based on the Wade−Mingos−Lauher rule.[59] Therefore, two of the metal−metal bonds in the cluster are expected to have metal−metal double bond character. The apex Fe(2) of the M_5 pyramid is located at distances of 2.7580(8) and 2.7366(8) Å from Mo(1) and Mo(2), respectively. These bond distances are similar to those found in other Mo/Fe/S clusters and marginally indicate Mo−Fe single bonds. The apical Fe(2) atom also is located at distances of 2.4683(9) and 2.4721(9) Å from Fe(1) and Fe(3), respectively. These Fe−Fe bonds are the shortest among those found in other Mo/Fe/S clusters except perhaps in the nitrogenase FeMoco. There are a few examples in biologically important clusters with very short Fe−Fe distances such as peroxodiferric ferritin (2.53 Å)[60] and possibly the intermediate Q from MMO (2.46 Å)[61] in which the Fe atoms have high oxidation states of +3 or +4 with μ-oxo or μ-dioxo bridging ligands. In organometallic cluster,[62] Fe−Fe distances of compounds with Fe−Fe triple bonds are found between 2.177(3) and 2.34 Å and those with Fe−Fe double bonds are found between 2.215 and 2.326(4) Å. Compounds having Fe−Fe double bonds, as a result of coordination unsaturation, of the type $Fe_2(CO)_5(\mu\text{-}PR_2)$, show Fe−Fe distances between 2.46 and 2.48 Å.[63] The distances of 2.4683(9) and 2.4721(9) Å found in **X** are shorter than the Fe−Fe distance in metallic iron (2.48 Å) and appear between the distances in Fe−Fe single and double bonds. The Mo atoms show very short Mo−Fe distances to other Fe atoms at 2.5763(7), 2.6279(8), 2.6127(8), and 2.6308(8) Å (Mo(1)−Fe(1), Mo(1)−Fe(3), Mo(2)−Fe(1), and Mo(2)−Fe(3), respectively). These values are shorter than those in **IIIa** and the bonds are considered as Mo−Fe bonds. The Mo(1)−Fe(1) bond distance of 2.5763(7) is shorter than the Mo(2)−Fe(1) bond (2.6127(8) Å).

The $[MoFe_3S_3]$ moiety of **X** mimics the core structure of the Roussin-salt like $[MoFe_3S_3]^{2+}$ compounds[33] with an isosceles triangular Fe_3 arrangement. The two shorter distances among the three Fe−Fe distances in the Roussin-salt type $[MoFe_3S_3]^{2+}$ compounds are found in the range of 2.6248(11) to 2.7193(7) Å. Those in the $(Cl_4\text{-cat})_2Mo_2Fe_3S_5(PEt_3)_5$ cluster (X) are 2.4683(9) and 2.4721(9) Å.

Mössbauer Spectroscopy and Magnetic Studies. The Mössbauer parameters for **I** at $\delta = 0.43$ mm/s and $\Delta E_Q = 1.47$ mm/s are similar to those of $(Et_4N)_2[S_2MoS_2Fe(SPh)_2]$ ($\delta = 0.45$ mm/s and $\Delta E_Q = 1.96$ mm/s)[64] and indicate similar oxidation states for the Fe centers. The magnetic susceptibility of $(Et_4N)_2[(Cl_4\text{-cat})MoOS_2FeCl_2]$ (**I**) (4.741 μ_B at 5 K and 5.413 μ_B at 300 K) indicates weak antiferromagnetic interactions between the metal centers, ($S = 1/2$ Mo(V) and $S = 5/2$ Fe(III)). The room-temperature magnetic moment is very similar to the value of 5.3 μ_B reported for $(Et_4N)_2[S_2MoS_2FeCl_2]$.[65] On the basis of the magnetic and Mössbauer data, the Mo and Fe centers in **I** are best described in terms of roughly equal admixtures of the Mo^V-Fe^{III} and Mo^{VI}-Fe^{II} formal oxidation states. The irreversible reduction potential of compound **I** at −1.1V in MeCN hints of the possible formation of a new cluster after reduction and reductive coupling.

Table 4. Mössbauer Parameters for the $(Cl_4\text{-cat})_2Mo_2Fe_6S_8(PR_3)_6$ [R = Et (**IIIa**), ^{n}Pr (**IIIb**), ^{n}Bu (**IIIc**)] Clusters Measured at 125 K in Zero Applied Magnetic Field. The Source Was ^{57}Co in a Rh Matrix, and the Isomer Shift Was Reported versus Fe Metal at Room Temperature

compound	isomer shift, δ (mm/s)	quadrupole splitting, ΔE_Q (mm/s)
IIIa	0.47	0.98
IIIb	0.43	0.97
IIIc	0.40	0.90

The cluster **IIIa** with edge-linked $[MoFe_3S_4]^{2+}$ reduced cores shows magnetic susceptibility of 7.42 μ_B at 300 K and 5.05 μ_B at 4 K. The ambient-temperature magnetic moments have established $S = 3/2$ and $S = 2$ states for the $[MoFe_3S_4]^{3+}$and $[MoFe_3S_4]^{2+}$ clusters, respectively.[66] In **IIIa** (with two coupled $[MoFe_3S_4]^{2+}$ subunits), the 300 K magnetic moment of 7.42 μ_B is smaller than the spin-only moment expected for a $S = 4$ spin system (8.94 μ_B). The results imply antiferromagnetic coupling in **IIIa**. Such antiferromagnetic coupling is also apparent in the magnetic moment of **IIIc** which is 5.02 μ_B at 300K and 4.42 μ_B at 4K.

Mössbauer measurements for $(Cl_4\text{-cat})_2Mo_2Fe_6S_8(PR_3)_6$ [R = Et (**IIIa**), ^{n}Pr (**IIIb**), ^{n}Bu (**IIIc**)] at 125 K show the influence of the phosphine ligands on the electronic property of the Fe centers. Trialkylphosphines are electron-rich and considered σ-donor/π-acceptor ligands. The isomer shift moves to the negative direction as the length of the alkyl chains increases and average isomer shifts and quadrupole splitting for $(Cl_4\text{-cat})_2Mo_2Fe_6S_8(PR_3)_6$ [R = Et (**IIIa**), ^{n}Pr (**IIIb**), ^{n}Bu (**IIIc**)] are shown at Table 4. This change indicates that the Fe formal oxidation state increases as the electron releasing effect on the phophine ligand increases. Such phenomena are reflected in minor structural changes among **IIIa**, **IIIb**, and **IIIc**. The Mo−P bond length changes (see above) suggest that the Mo-bound PR_3 ligands act as σ-donors. The Fe atoms, however, based mainly on the Mössbauer data, appear to back-bond to the P donor atoms, and the Fe-bound PR_3 ligands serve as π-acceptors. The latter withdraw more *d* electron density from the Fe centers as the alkyl chain length (and P → Fe σ bonding) increases.

The Mössbauer measurement for $(Et_4N)[Fe(PEt_3)Cl_3]$ (**VI**) was carried out at 125 K and the spectrum showed a typical high spin Fe(II) center (Figure 11A). A series of FeL_2X_2 and $FeLX_3^-$ (L = neutral ligand, X = Cl, Br, I) compounds have been investigated by Mössbauer spectroscopy at room temperature,[67] and a similar $(Et_4N)[Fe(Quinoline)Cl_3]$ complex shows a doublet of $\delta = 0.88$ mm/s and $\Delta E_Q = 2.08$ mm/s. The parameters for $(Et_4N)_2[FeCl_4]$,[66] $(Et_4N)[Fe(PEt_3)Cl_3]$ (**VI**),[7(d)] and $Fe(PEt_3)_2Cl_2$ are shown at Table 5. The isomer shift decreases, and the quadrupole splitting increases as the number of PEt_3 increases. A decrease in the number of chloride ligands

(59) Lauher, J. W. *J. Am. Chem. Soc.* **1978**, *100*, 5305.
(60) Hwang, J.; Krebs, C.; Huynh, B. H.; Edmondson, D. E.; Theil, E. C.; Penner-Hahn, J. E. *Science* **2000**, *287*, 122.
(61) Shu, L. J.; Nesheim, J. C.; Kauffmann, K.; Münck, E.; Lipscomb, J. D.; Que, L. *Science* **1997**, *275*, 515.
(62) Cotton, F. A. *Chem. Soc. Rev.* **1975**, *4*, 27.
(63) Cotton, F. A.; Wilkinson, G.; Murillo, C. A.; Bochmann, M. *Advanced Inorganic Chemistry*, 6th ed.; Wiley-Interscience: New York, 1999; p 795 and references therein.
(64) (a) Coucouvanis, D.; Baenziger, N. C.; Simhon, E. D.; Stremple, P.; Swenson, D.; Kostikas, A.; Simopoulos, A.; Petrouleas, V.; Papefthymiou, V. *J. Am. Chem. Soc.* **1980**, *102*, 1730.
(65) (a) Coucouvanis, D.; Stremple, P.; Simhon, E. D.; Swenson, D.; Baenziger, N. C.; Draganjac, M.; Chan, L. T.; Simopoulos, A.; Papaefthymiou, V.; Kostikas, A.; Petrouleas, V. *Inorg. Chem.* **1983**, *22*, 293. (b) Simopoulos, A.; Papaefthymiou, V.; Kostikas, A.; Petrouleas, V.; Coucouvanis, D.; Simhon E. D.; Stremple, P. *Chem. Phys. Lett.* **1981**, *81*, 261. (c) Coucouvanis, D.; Simhon, E. D.; Swenson, D.; Baenziger, N. C. *J. Chem. Soc., Chem. Commun.* **1979**, 361.
(66) Mascharak, P, K.; Papaefthymiou, G. C.; Armstrong, W. H.; Foner, S.; Frankel, R. B.; Holm, R. H. *Inorg. Chem.* **1983**, *22*, 2851.
(67) Burbridge, C. D.; Goodgame, D. M. L. *J. Chem. Soc. (A)* **1968**, 1074.

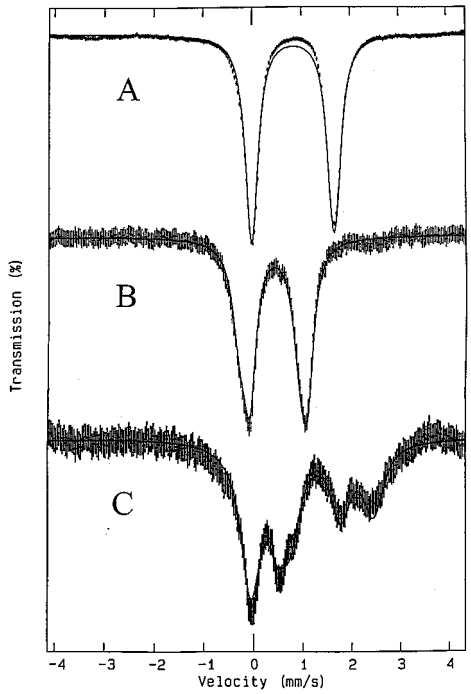

Figure 11. ^{57}Fe Mössbauer spectrum of $(Et_4N)[Fe(PEt_3)Cl_3]$ **(VI)** in A, $[(Cl_4\text{-cat})_2Mo_2Fe_2S_3O(PEt_3)_3Cl]\cdot 1/2(Fe(PEt_3)_2(MeCN)_4)$ **(VIII)** in B, and $(Cl_4\text{-cat})_2Mo_2Fe_3S_5(PEt_3)_5$ **(X)** in C measured at 125 K in zero applied magnetic field. The source was ^{57}Co in a Rh matrix, and the isomer shift was reported versus Fe metal at room temperature. The cross marks are for the observed data, and the solid line shows the simulated graph fitted with one Fe center. The high signal-to-noise ratio appeared in **C** is due to the unavailability of the compound in sufficient amount.

Table 5. Mössbauer Parameters for $[Fe(II)(PEt_3)_nCl_{(4-n)}]^{(2-n)+}$, ($n$ = 0−2) Monomer in Zero Applied Magnetic Field

compound	isomer shift, δ (mm/s)	quadrupole splitting, ΔE_Q (mm/s)	temp (K)
$(Et_4N)_2[FeCl_4]^a$	0.90	0.76	293
$(Et_4N)[Fe(PEt_3)Cl_3]$ **(VI)**	0.84	1.68	125
$Fe(PEt_3)_2Cl_2{}^b$	0.65	2.90	200

[a] Reference 67. [b] Reference 7d.

(strong σ-donors) may explain these data, although the possibility of weak π-accepting by the PEt_3 ligand cannot be ruled out.

The $[Mo_2Fe_2S_3O]^{4+}$ unit of the $[(Cl_4\text{-cat})_2Mo_2Fe_2S_3O(PEt_3)_3Cl]\cdot 1/2(Fe(PEt_3)_2(MeCN)_4)$ cluster (**VIII**) can be described in terms of various different formal oxidation states for the metal ions: $[Mo^{IV}{}_2Fe^{II}{}_2]$, $[Mo^{III}Mo^{IV}Fe^{II}Fe^{III}]$, and $[Mo^{III}{}_2Fe^{III}{}_2]$. The Mössbauer spectrum (Figure 11B) of **VIII** shows a quadrupole doublet at 125 K that can be fitted assuming three Fe centers with δ = 0.386, 0.365, 0.464 mm/s and ΔE_Q = 0.999, 1.355, 1.155 mm/s, respectively. The Mössbauer study of hexacoordinate porphyrin complexes with phosphorus axial ligands indicates that most iron centers of this type are low-spin Fe(II) with the parameters of δ = 0.26−0.41 mm/s and ΔE_Q = 0.35−0.86 mm/s over various temperatures.[68] In **VIII**, the quadrupole doublet of δ = 0.365 mm/s and ΔE_Q = 1.355 mm/s is assigned to the $[Fe^{II}(PEt_3)_2(MeCN)_4]^{2+}$ counterion and is similar to the quadrupole doublet found for the independently synthesized **IX** (δ = 0.368 mm/s; ΔE_Q = 1.097 mm/s).

The other two quadrupole doublets in **VIII** are due to the two Fe centers in the cuboidal unit and appear to indicate a valence-localized structure. An all-ferrous description with a $Mo^{IV}{}_2Fe^{II}{}_2$ core can be ruled out since for such a description larger isomer shift values would be expected. The Fe(II)-PR_3 site in the $[Fe_4S_4]^+$ cubanes usually shows an isomer shift between δ = 0.41−0.56 mm/s under the same conditions.[8,69] The effect of the oxygen atom in the Mössbauer spectrum of the $[Mo_2Fe_2S_3O]^{4+}$ cluster of **VIII** can be deduced from data available for other known compounds. The isomer shift of $(Ph_4P)_2[Fe_4S_4(SPh)_4]$ is found at δ = 0.43 mm/s at 77 K.[70] The phenolate cluster, $(Et_4N)_2[Fe_4S_4(OPh)_4]$, shows δ = 0.50 mm/s at 4.2 K and a positive shift in the ^{57}Fe isomer shift values (ca. 0.07 mm/s).[71] Similarly, the Mössbauer spectra for the $[Fe_6S_6]^{3+}$ clusters at 125 K[9c] show isomer shifts at δ = 0.440 mm/s for $(Et_4N)_3[Fe_6S_6(S\text{-}p\text{-}MeC_6H_4)_6]$, and δ = 0.476 mm/s for the O-p-MeC_6H_4 analogue, which is a more positive shift by 0.036 mm/s. Therefore, the Fe atom in the $FePOS_2$ center may be expected to have a more positive δ value than that in the $FePS_3$ center. Formally, the doublet of δ = 0.386 mm/s and ΔE_Q = 0.999 mm/s is then assigned to the Fe(1)−Cl site with an Fe(III) oxidation state. The Fe(2)−P site, with δ = 0.464 mm/s and ΔE_Q = 1.155 mm/s, is assigned to an Fe(II) oxidation state. EPR measurements of **VIII** in CH_2Cl_2 glass at 110 K did not show a substantial signal, and the even number electrons in the cluster and cation were confirmed. The magnetic and Mössbauer data combined lead to the assignment $Mo^{III}Mo^{IV}Fe^{II}Fe^{III}$ for the oxidation states of the core metal ions in **VIII**. The magnetic moments for **VIII** at 7.95 μ_B (300 K) and 5.33 μ_B (4 K) are consistent with a weakly, antiferromagnetically coupled S = 4 spin-only system (8.94 μ_B).

The Mössbauer spectrum of the $(Cl_4\text{-cat})_2Mo_2Fe_3S_5(PEt_3)_5$ cluster (**X**) obtained on a few crystals at 125 K was fitted with three sets of quadrupole doublets and indicates that all Fe atoms are high spin: δ = 0.34 mm/s, 1.12 mm/s, 1.19 mm/s and ΔE_Q = 0.81 mm/s, 1.29 mm/s, 2.51 mm/s, respectively (Figure 11C). The isomer shifts imply that the compound has one Fe(III) and two Fe(II) centers. Unusually large isomer shifts and quadrupole splitting of the Fe(II) centers as in **X** are also found in the reduced $[Fe_4S_4]^0$ cluster in the Fe protein of nitrogenase.[72] The $[Fe_4S_4]^0$ cluster in the Fe protein showed very short Fe−Fe distances of 2.52 Å from EXAFS measurement,[73] and the recent protein X-ray crystallography also showed the presence of 2.54 and 2.57 Å Fe−Fe distances.[74] In **X**, Fe(1) and Fe(3) are believed to be high spin ferrous centers and Fe(2) to be a high spin ferric center. The two ferrous iron centers are related by the approximate mirror plane that contains Mo(1), Fe(2), and Mo(2) atoms and show almost the same isomer shifts. The difference in quadrupole splitting between Fe(1) and Fe(II) is difficult to explain.

The magnetic susceptibility of **X** was measured over various temperatures, and it showed a maximum magnetic moment of 10.96 μ_B at 95 K (Figure 12). The magnetic moment decreases slowly to 9.10 μ_B when the temperature increases from 115 K to 325 K. Below 95 K, the magnetic moment decreases steeply

(68) Ohya, T.; Morohoshi, H.; Sato, M. *Inorg. Chem.* **1984**, *23*, 1303.
(69) Tyson, M. A.; Coucouvanis, D. Unpublished results.
(70) Evans, D. J.; Hills, A.; Hughes, D. L.; Leigh, G. J. *J. Chem. Soc., Dalton Trans.* **1990**, 2753.
(71) (a) Cleland, W. E.; Holtman, D. A.; Sabat, M.; Ibers, J. A.; DeFotis, G. C.; Averill, B. A. *J. Am. Chem. Soc.* **1983**, *105*, 6021. (b) Kanatzidis, M. D.; Baenziger, N. C.; Coucouvanis, D.; Simopoulos, A.; Kostikas, A. *J. Am. Chem. Soc.* **1984**, *106*, 4500.
(72) Yoo, S. J.; Angove, H. C.; Burgess, B. K.; Hendrich, M. P.; Münck, E. *J. Am. Chem. Soc.* **1999**, *121*, 2534.
(73) Musgrave, K. B.; Angove, H. C.; Burgess, B. K.; Hedmann, B.; Hodgson, K. O. *J. Am. Chem. Soc.* **1998**, *120*, 5325.
(74) Strop, P.; Takahara, P. M.; Chiu, H.-J.; Angove, H. C.; Burgess, B. K.; Rees, D. C. *Biochemistry* **2001**, *40*, 651.

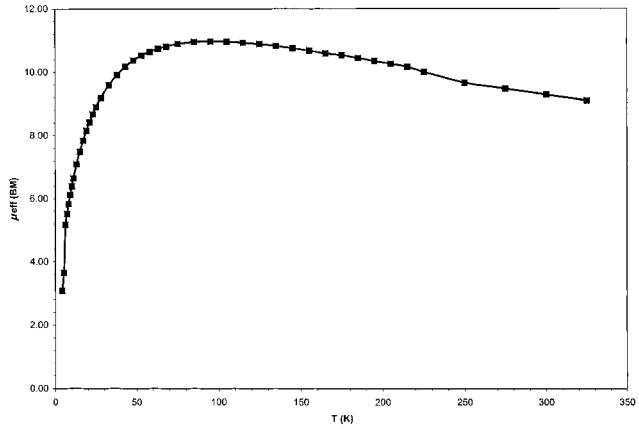

Figure 12. Molar magnetic susceptibility of $(Cl_4\text{-cat})_2Mo_2Fe_3S_5(PEt_3)_5$ cluster (**X**) plotted μ_{eff} versus temperature.

to 3.08 μ_B (4 K) and shows strong antiferromagnetic coupling. The maximum μ_{eff} of 10.96 μ_B corresponds to the magnetic moment of the $S = 5$ spin-only system. On the basis of the Mössbauer measurements (at 125 K), the oxidation state of the metal atoms can be assigned as $Mo^{III}Mo^{IV}Fe^{II}_2Fe^{III}$, and the Fe atoms of the compound seem to have $S = 2$, 2, and 5/2, respectively. At present the coupling of the Fe triad to the two Mo atoms and the onset of antiferromagnetism at temperatures <50 K has not been delineated. An analysis of the magnetic data is currently in progress and will be reported in a future publication.

Summary

The synthesis of multimetallic M/S clusters by the reductive coupling of dimeric building blocks appears to be of general utility. Under reducing conditions, dinuclear clusters with coordinatively unsaturated cores such as $[Fe_2S_2]^{2+}$, $[MoFeS_2]^{4+}$, and $[MoFeSO]^{4+}$ couple to give cluster products with cores such as $[Fe_4S_4]^{2+}$, $[MoFe_3S_4]^{3+}$, $[MoFe_3S_3O]^{4+}$, and $[MoFe_3S_4]^{2+}$. The synthesis of $[Fe_4S_4]^{2+}$ cluster from the reductive coupling of $[Fe_2S_2]^{2+}$ is well-known.[16] The general utility of this coupling reaction in the synthesis of heterometallic clusters, however, has not been previously reported.

In this paper we report for the first time the synthesis by reductive coupling of clusters with the $[MoFe_3S_4]^{3+}$ cores (**VIIa** and **VIIb**), the $[MoFe_3S_4]^{2+}$ cores (**IIIa**, **IIIb**, and **IIIc**), and the $[Mo_2Fe_2S_3O]^{4+}$ cores (**VIII**). The reductive coupling synthesis of clusters with the $[Mo_2Fe_2S_4]^{4+}$ cores also has been achieved.[75]

This type of reductive coupling reactions combined with conditions that favor the removal of terminal ligands may be necessary for the synthesis of polynuclear clusters with a minimum of terminal ligands, and extensive bridging by core sulfido ligands. The P clusters and the FeMoco of nitrogenase are two such clusters for which there exist no synthetic analogues. At present we are exploring the synthesis of such clusters by the reductive coupling of appropriate smaller building blocks.

Acknowledgment. The authors acknowledge the support of this work by a grant from the National Institutes of Health (GM 33080). Dr. Namdoo Moon in the Biophysics Department at the University of Michigan is greatly appreciated for his Mössbauer and EPR measurements and helpful discussion.

Supporting Information Available: The X-ray crystallographic file in CIF format for $(Cl_4\text{-cat})_2Mo_2Fe_6S_8(P^nBu_3)_6$ (**IIIc**), $(PF_6)[Fe_6S_8(P^nPr_3)_6]$ (**V**), $(Et_4N)[Fe(PEt_3)Cl_3]$ (**VI**), $(Et_4N)_2[(Cl_4\text{-cat})Mo(L)Fe_3S_4Cl_3]$ [L = MeCN (**VIIa**), THF (**VIIb**)], $[(Cl_4\text{-cat})_2Mo_2Fe_2S_3O(PEt_3)_3Cl]\cdot 1/2(Fe(PEt_3)_2(MeCN)_4)$ (**VIII**), $(BPh_4)_2[Fe(PEt_3)_2(MeCN)_4]$ (**IX**), and $(Cl_4\text{-cat})_2Mo_2Fe_3S_5(PEt_3)_5$ (**X**) (PDF). This material is available free of charge via the Internet at http://pubs.acs.org.

IC0104914

(75) Han, J.; Coucouvanis, D. *J. Am. Chem. Soc.*, in press.